AD-A160 838 STUDY OF FAN-AIRPUMP APPLICABILITY TO TWO-STAGE AIR CLEANER SYSTEMS(U) SOUTHWEST RESEARCH INST SAN ANTONIO TX M B TREUHAFT JUN 85 SRRI-03-8070 TACOM-TR-13110 1/1

UNCLASSIFIED DAAE07-84-C-R045 F/G 13/1 NL

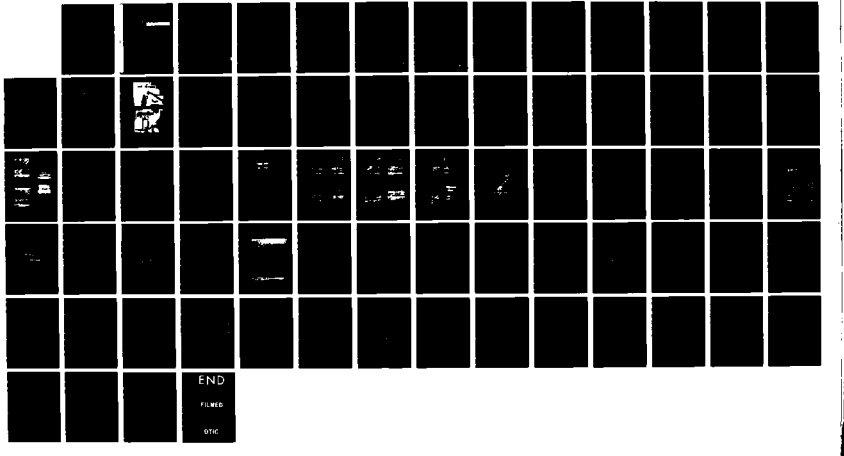

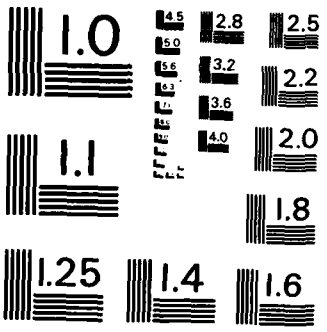

(12)

R and D CENTER

LABORATORY

TECHNICAL REPORT

NO. 13118

STUDY OF FAN-AIRPUMP APPLICABILITY TO TWO-STAGE AIR CLEANER SYSTEMS

CONTRACT NO. DAAE07-84-C-R045

JUNE 1985

Martin B. Treuhaft
Southwest Research Institute
6220 Culebra Road
by San Antonio, TX 78284

U.S. ARMY TANK-AUTOMOTIVE COMMAND
RESEARCH AND DEVELOPMENT CENTER
Warren, Michigan 48397-5000

NOTICES

This report is not to be construed as an official Department of the Army position.

Mention of any trade names or manufacturers in this report shall not be construed as an official indorsement or approval of such products or companies by the U.S. Government.

Destroy this report when it is no longer needed. Do not return it to the originator.

SECURITY CLASSIFICATION OF THIS PAGE

REPORT DOCUMENTATION PAGE

AD-A160 835

1a REPORT SECURITY CLASSIFICATION Unclassified	1b. RESTRICTIVE MARKINGS
2a SECURITY CLASSIFICATION AUTHORITY	3. DISTRIBUTION/AVAILABILITY OF REPORT Approved for public release; Distribution unlimited
2b DECLASSIFICATION/DOWNGRADING SCHEDULE	
4 PERFORMING ORGANIZATION REPORT NUMBER(S) 03-8070	
6a NAME OF PERFORMING ORGANIZATION Southwest Research Institute	6b. OFFICE SYMBOL (If applicable)
6c. ADDRESS (City, State, and ZIP Code) 6220 Culebra San Antonio, Texas 78284	7a. NAME OF MONITORING ORGANIZATION 7b. ADDRESS (City, State, and ZIP Code)
8a. NAME OF FUNDING/SPONSORING ORGANIZATION U.S. Army Tank-Automotive Command	8b. OFFICE SYMBOL (If applicable) DRSTA-RGT
8c. ADDRESS (City, State, and ZIP Code) Warren, Michigan 48397-5000	9. PROCUREMENT INSTRUMENT IDENTIFICATION NUMBER

10. SOURCE OF FUNDING NUMBERS			
PROGRAM ELEMENT NO.	PROJECT NO.	TASK NO.	WORK UNIT ACCESSION NO.
-			

11. TITLE (Include Security Classification)
Study of Fan-Airpump Applicability to Two-Stage Air Cleaner Systems

12. PERSONAL AUTHOR(S) Martin B. Treuhaft

13a. TYPE OF REPORT	13b. TIME COVERED	14. DATE OF REPORT (Year, Month, Day)	15. PAGE COUNT
Final	FROM _____ TO _____	1985, June	

16. SUPPLEMENTARY NOTATION

17 COSATI CODES			18. SUBJECT TERMS (Continue on reverse if necessary and identify by block number)
FIELD	GROUP	SUB-GROUP	Air cleaners, Aspirators, Scavenge airflow, Dust removal, Dust capacity.

19. ABSTRACT (Continue on reverse if necessary and identify by block number)

An experimental program was conducted to evaluate applicability of the fan-airpump concept as applied to military air cleaner systems and vehicles. Technical feasibility and potential use were evaluated through laboratory testing which defined fan-airpump performance characteristics and investigated the performance envelope of the fan-airpump concept when applied to the 2-1/2 and 5-ton truck. Economic feasibility was assessed by comparing projected fan-airpump life cycle cost factors with similar cost factors associated with blower motor systems. Because it has no moving parts, requires no lubrication, and is practically maintenance, free, the use of a fan-airpump to develop the scavenge flows required by two-stage air cleaner systems would alleviate the problems caused by unreliable blower motors or marginal exhaust aspirator replacements. As a result, the fan-airpump could become a major component for improving reliability and operational readiness for many vehicles operating with two-stage air cleaner systems.

20 DISTRIBUTION/AVAILABILITY OF ABSTRACT	21. ABSTRACT SECURITY CLASSIFICATION	
☒ UNCLASSIFIED/UNLIMITED ☐ SAME AS RPT ☐ DTIC USERS	Unclassified	
22a NAME OF RESPONSIBLE INDIVIDUAL Frank Margrif /G. Khalil	22b. TELEPHONE (Include Area Code) 313/574-5185	22c. OFFICE SYMBOL AMSTA-RTG

DD FORM 1473, 84 MAR 83 APR edition may be used until exhausted
All other editions are obsolete

SECURITY CLASSIFICATION OF THIS PAGE
UNCLASSIFIED

PREFACE

The author wishes to thank Buddy Kremer for his contribution during testing and Terry Edwards for her help in preparing this report.

A-1

TABLE OF CONTENTS

LIST OF ILLUSTRATIONS

LIST OF ILLUSTRATIONS (Continued)

LIST OF ILLUSTRATIONS (Continued)

LIST OF ILLUSTRATIONS (Continued)

LIST OF TABLES

1.0. INTRODUCTION

This final technical report, prepared by Southwest Research Institute, for the U.S. Army Tank-Automotive Command (TACOM) under Contract DAAE07-84-C-R045, describes an experimental program to evaluate applicability of the fan-airpump concept as applied to military air cleaner systems and vehicles. Technical feasibility and potential use were evaluated through laboratory testing which defined fan-airpump performance characteristics and investigated the performance envelope of the fan-airpump concept when applied to the 2½- and 5-ton truck. Economic feasibility was assessed by comparing projected fan-airpump life cycle cost factors with similar cost factors associated with blower motor systems. Because it has no moving parts, requires no lubrication, and is practically maintenance free, the use of a fan-airpump to develop the scavenge flows required by two-stage air cleaner systems would alleviate the problems caused by unreliable blower motors or marginal exhaust aspirator replacements. As a result, the fan-airpump could become a major component for improving reliability and operational readiness for many vehicles operating with two-stage air cleaner systems.

2.0. OBJECTIVES

The primary objectives of this program were to study, analyze, and perform laboratory tests to determine the applicability of the fan-airpump concept for two-stage air cleaner systems for military vehicles.

3.0. CONCLUSIONS

3.1. Fan-Airpump Feasibility

The fan-airpump concept provides a feasible, cost-effective alternative for developing secondary airflows for two-stage air cleaner systems, and when optimized should be applicable to several classes of military vehicles.

3.2. Applicability to 2½-Ton Truck

Integration of a properly designed precleaner into the 2½-ton truck air cleaner system will significantly improve service life. Secondary airflow for this system can be provided by a fan-airpump.

3.3. Component Integration on the 2½- and 5-Ton Truck

Underhood airflow development by the radiator fan is favorable for easy component installation near the air cleaner housing. This proximity simplifies duct design and assures that only minor flow losses will be experienced in connecting the secondary port to the air cleaner.

3.4. Engine Cooling

Because the fan-airpump can be installed so that it does not remove air from the engine compartment, it should have little or no effect on engine cooling.

Consideration should be given to design and placement to assure that dust ejection does not interfere with heat exchanger operation.

3.5. Secondary Airflow Requirement

Maintaining scavenge flow equal to 10 percent of the primary airflow, as is common practice, may not be necessary for effective precleaner operation. While the range of this parameter was not studied or defined, operation with scavenge flows as low as 5 percent provided successful operation on a modified 2½-ton truck system.

3.6. Secondary Airflow Development and Duct Design

Secondary flow development was effected most by sharp 90-degree bends and duct roughness.

3.7. Service Life

Overall service life is very sensitive to precleaner efficiency provided the pressure drop penalty for incorporating the precleaner is not severe. Dust loading for the final filter with respect to the new particle size distribution must be considered and some redesign is likely for system optimization.

3.8. Cost Benefit Assessment

The fan-airpump offers a significant cost savings compared with blower motor systems. These savings result from lower initial and operating costs.

3.9. Reliability

Because it has no moving parts to wear out or fail, the fan-airpump system will require minimium maintenance and will significantly improve operational readiness compared to blower motor systems.

3.10. Engine Performance

The fan-airpump will have no adverse effect on engine performance as is often the case with exhaust system aspirators which affect exhaust backpressure.

4.0. RECOMMENDATIONS

4.1. Testing

Further testing should be conducted to define on-vehicle performance and to determine optimum fan-airpump design for the 2½-ton truck. Total system design, including the precleaner, should be considered.

4.2. 5-Ton Truck

The aircleaner system for the 5-ton truck should be analyzed to determine if design changes can be made to take advantage of secondary flow to increase overall service life.

4.3. Other Vehicles

In addition to the 2½- and 5-ton trucks, other vehicles should be analyzed for fan-airpump applicability.

5.0. DISCUSSION

5.1. Introduction

To achieve satisfactory collection efficiency and service life, many two-stage air cleaners operate with a scavenged precleaner. This is necessary to avoid dust reentrainment, maximize precleaner separation efficiency, and extend service life to acceptable limits. In many cases, the scavenge flow is developed by electrically driven blowers, usually designed to give 10 percent of the air cleaner's rated capacity. A common installation is shown in Figure 5-1.

A major problem with this type of system is the tendency for premature blower motor failure. A recent study showed the mean operating time to failure for blower motor assemblies used on many Army vehicles was only 25 to 60 percent of the minimum specified requirement. This reduced operational readiness and required a high expenditure of money and manpower to maintain air cleaner operability. Because of these failures, alternate means for providing scavenge air have been and continue to be considered. As a result, some product improvement programs have already been undertaken, for instance the replacement of blower motors with exhaust-driven aspirators on M60-series tanks.

It is unlikely, however, that exhaust gas aspiration can solve all blower motor problems. In fact, there are many situations where exhaust gas aspirators are neither appropriate nor practical. For example, when the physical arrangement of the vehicle requires the aspirator to be located some distance from the air cleaner, with numerous bonds in the ducting the scavenge flows will often be too weak for effective precleaner operation. The fan-airpump concept, illustrated in Figure 5-2, could solve this problem because it uses the aspiration principle in a different way. The fan-airpump itself is a specially designed aspirator that attaches near the radiator fan shroud, usually within good proximity to the air cleaner. A fraction of the fan's airflow enters the inlet and is forced through a nozzle where it is converted to a high-velocity stream. This decreases pressure in the suction chamber creating a partial vacuum to scavenge dust and dirt from the precleaner. Once air exits the aspirator, it is available for cooling as originally intended.

At present, fan-airpumps are being used on agricultural equipment as a major component in the cab air filtration system. Some typical fan-airpump installations are shown in Figure 5-3. Successful operation of these units in dusty farm

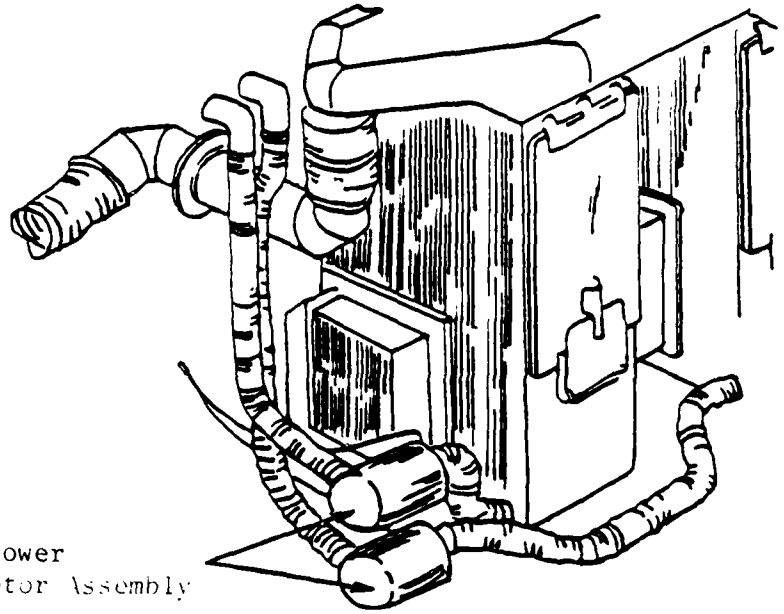

Figure 3-1. Typical Blower Motor Installation, M109 Howitzer[1]

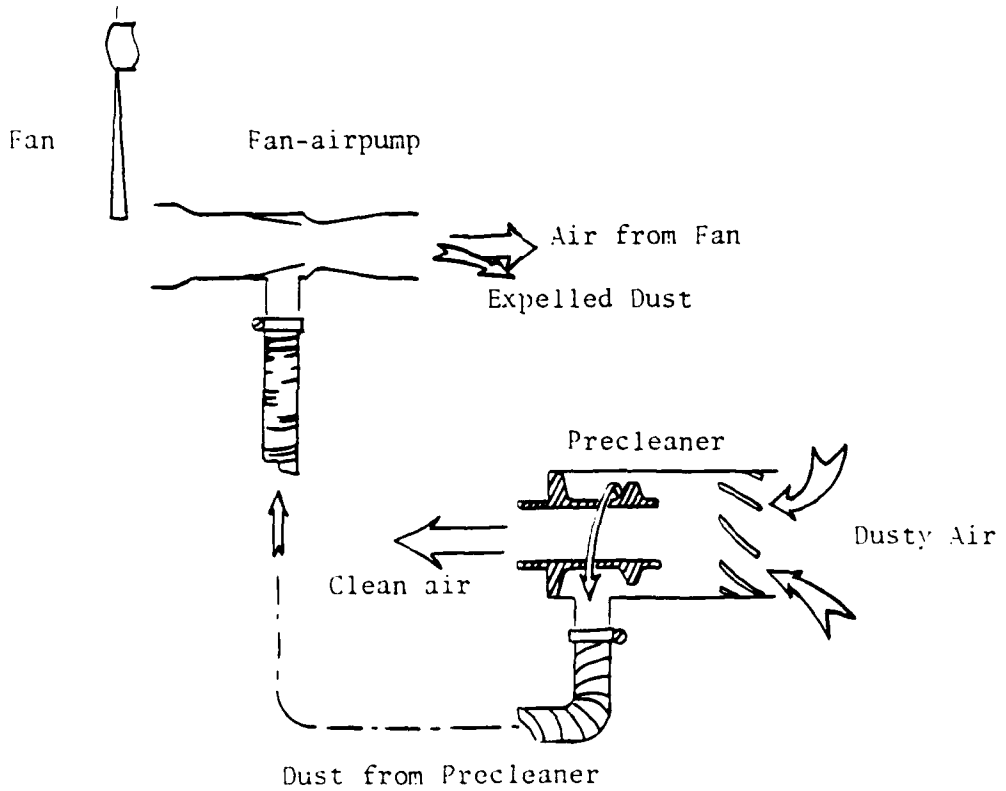

Figure 3-2. Schematic of Fan-Airpump Operation

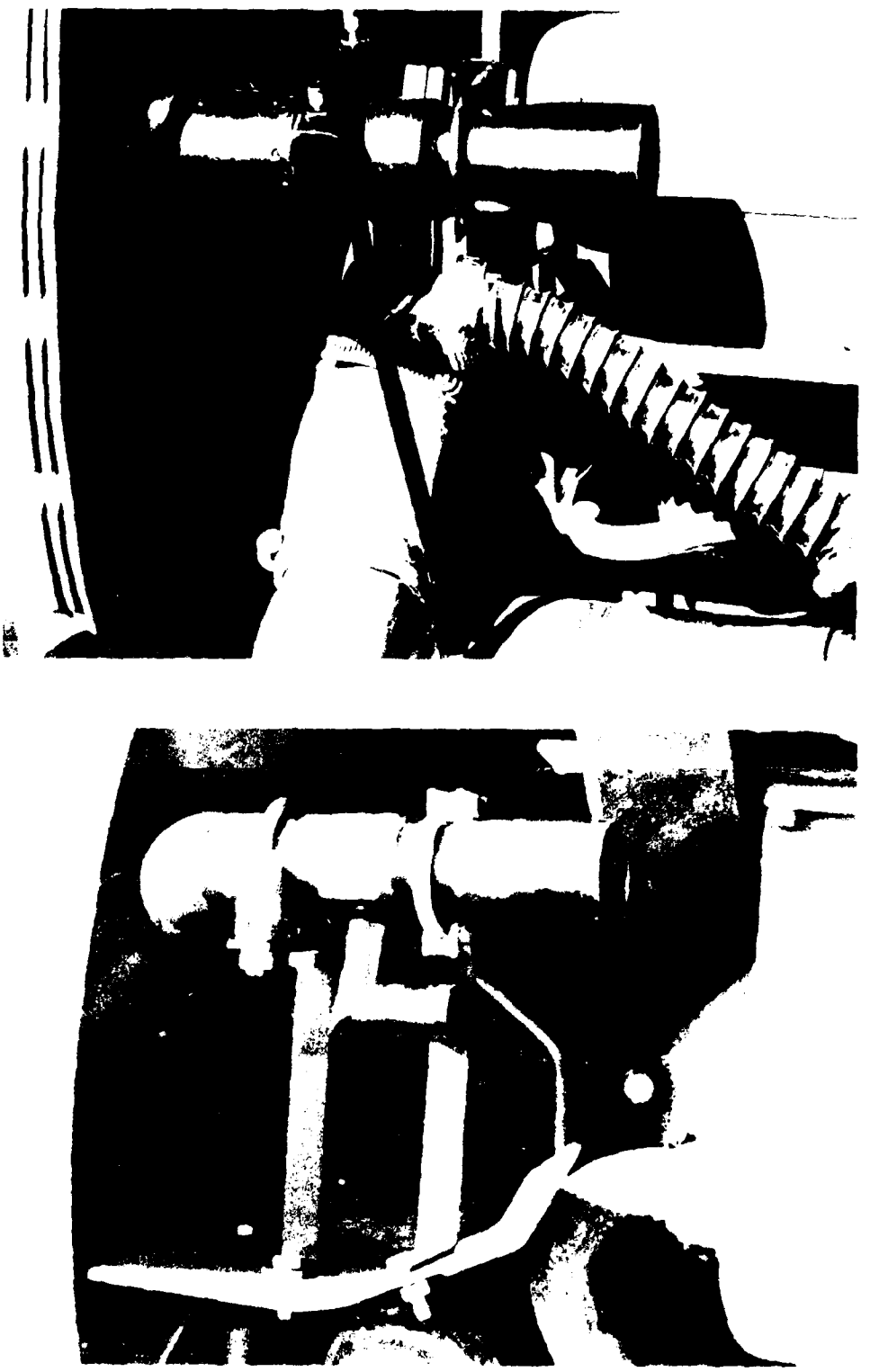

Figure 5-3. Fan-Airpump Installed on Agricultural Tractors

environments suggest their applicability for military vehicles. Furthermore, since they have no moving parts to wear out or fail, and since they will enjoy better proximity to the engine, fan-airpumps could offer a long term, cost-effective solution to the problems caused by unreliable blower motors and inadequate exhaust aspirators.

Recognizing these potential advantages, TACOM supported research to investigate fan-airpump applicability to military vehicles. For the most part, research was directed toward three areas: laboratory testing to define fan-airpump performance characteristics over a large range of operating conditions; analysis to compare laboratory performance with the operating requirements of military two-stage air cleaner systems; and experimental and theoretical analyses to measure the impact of ducting, fan orientation, and shroud design on secondary airflow development.

A design component and component integration study was also conducted for various 2½- and 5-ton trucks. During this study, airflow patterns in the engine compartment were mapped to indicate suitable locations for fan-airpump placement and to determine minimum ducting requirements for interfacing with the air cleaner system. Mapping was also conducted to assure that dust ejection would not enter the radiator or interfere with other engine components.

Finally, a cost-benefits analysis and economic assessment was conducted to compare the fan-airpump concept with other systems presently being used to provide precleaner scavenging. Particular attention was directed toward military vehicles using blower motors which, because of their moving parts, have been subject to wear-out and failure. Component cost, man-hour projections for retrofit, and life-cycle cost factors were considered.

5.2. Secondary Airflow Development

5.2.1. **Approach.** The first step in assessing fan-airpump potential is to characterize secondary flow development as a function of primary flow and with respect to fan-airpump orientation. These data are important because they define the range of possible scavenge flows, including the maximum flow, expected from a fan-airpump of given size and design when subjected to known upstream conditions. Measurements were made on four off-the-shelf units, described in Table 5-1, using the experimental set-up shown in Figure 5-4. The principal components used to measure flow were pitot tubes and laminar flow elements. Orientation with respect to the primary flow stream included direct coupling to the blower ($x = 0$), one- and two-inch separations ($\alpha = 0^{o}$), and centerline-to-centerline angular deviations of up to 60 degrees ($-60^{o} \leq \alpha \leq 60^{o}$; $x = 1 - 2$ inches). The general approach was to set the primary flow rate for a given fan-airpump orientation and then measure secondary flow development and primary and secondary pressures. The advantage of this procedure was that it provided direct comparison among several fan-airpump sizes, it established baseline data for comparison with on-vehicle measurements, and it generated a wide data base from which to assess fan-airpump potential.

Table 5-1. Fan-Airpump Dimensional Characteristics

Unit	A	B	C	D	E	F
1	2 3/8	2	1 3/8	8 3/4	1	4 5/8
2	2 3/4	2 1/2	1 5/8	9 3/4	1 1/2	4 1/8
3	3 1/2	3	2	10 1/2	1 1/2	4 1/4
4	2 3/4	2 1/2	1 5/8	9 5/8	1 1/2	4 1/8

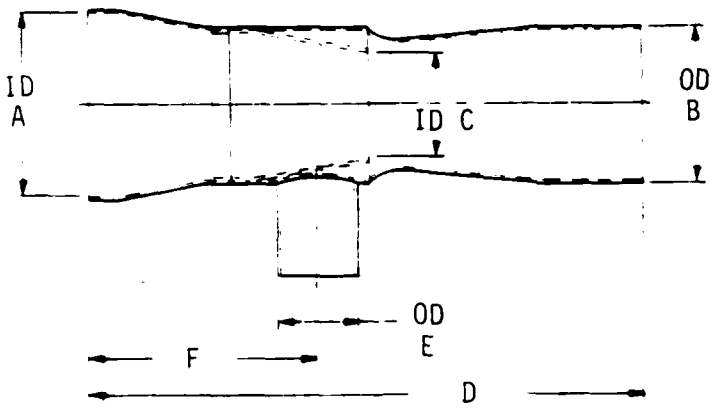

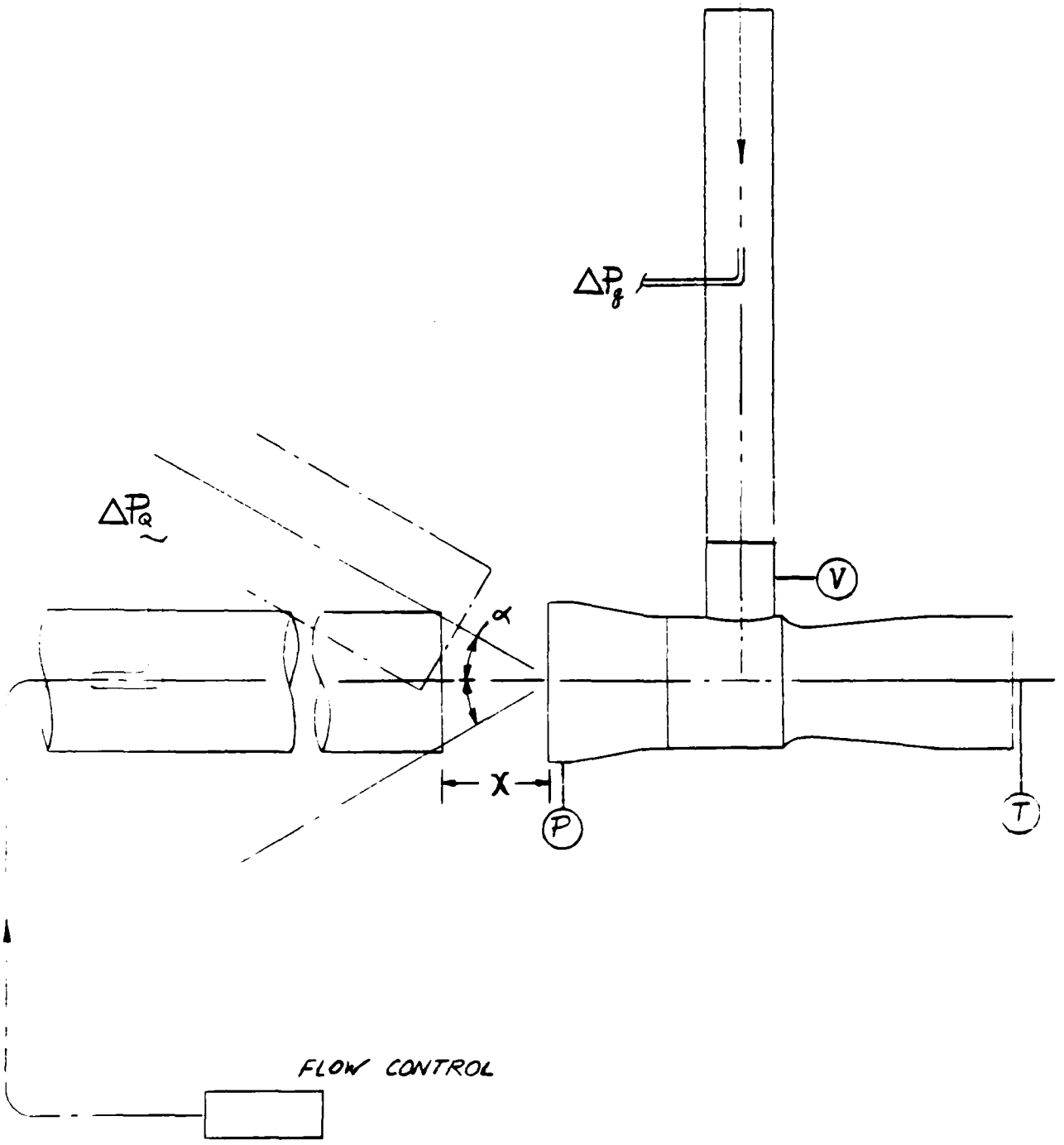

Figure 5-4. Experimental Arrangement for Measuring Secondary Flow Development

5.2.2. **Concentric Alignment.** In the first series of tests, each fan-airpump was concentrically aligned with the primary flow stream and the separation distance x between the fan-airpump and the source was incrementally set at 0 (directly coupled), 1, and 2 inches. This arrangement provided for different inlet conditions by geometrically altering the capture efficiency Γ of the fan-airpump. Measurements taken at x = 0 established baseline performance since capture efficiency for this case is 100 percent. For x greater than zero, free-stream performance was measured since the primary flow is not physically confined to the inlet (Γ<100 percent). All data were taken as a function of the primary flow rate Q.

Flows were calculated from centerline pitot tube data, corrected to give average velocity values based on the well-known relationship between the velocity ratio and Reynolds number, Figure 5-5. Results can be compared in several ways. Figures 5-6 through 5-13 show data for secondary airflow q, inlet static pressure P, and induced suction V and V_c as a function of the upstream flow Q, using logarithmic coordinates. The curves show that over a rather broad range of Q, secondary flow q for each unit can be correlated by a singular characteristic equation. These equations, which are discussed later, are given in Table 5-2.

Figures 5-14 to 5-17 show the ratio of the secondary to upstream flow q/Q as a function of Q. Figure 5-18 compares secondary flow development for unit 2 at x = 0, 1, and 2 inches, while similar curves for unit 3 are given in Figure 5-19. Figure 5-20 shows the ratio of the secondary flow at x to the secondary flow at x = 0, versus Q. The data clearly show the impact of separation distance on secondary flow development. As expected, for a given Q, values of q decrease with incremental spacing, particularly with respect to the baseline case (x = 0). This is due to lowered capture efficiency. It is important to note, that once decoupled (x>0), the impact of further incremental spacing within the short zone (x~2 - 3d) is less pronounced. This is because the behavior of the flow stream in this zone is similar to the behavior of a free jet. Momentum is nearly conserved, pressure and viscous effects are negligible, and boundary expansion is usually less than 24 degrees (included angle). For this situation, velocity at the centerline is substantially unchanged:

$$V_c/V_0 \approx 1 \tag{1}$$

When the expansion angle is fairly well known or can be reasonably assumed, velocities off the centerline can be calculated by:

$$3.3 \log \left[\frac{V_c}{V}\right] = \left[\frac{r}{r'}\right]^2 \tag{2}$$

where: r = radius from centerline to point of interest
r' = half the distance from the centerline to the jet boundary
V_c/V = ratio of centerline velocity to velocity at point of interest

This equation can be rearranged to give:

$$V = V_c 10^{-.3(r/r')^2} \tag{3}$$

which is useful in calculating specific velocity values at any point in the jet.

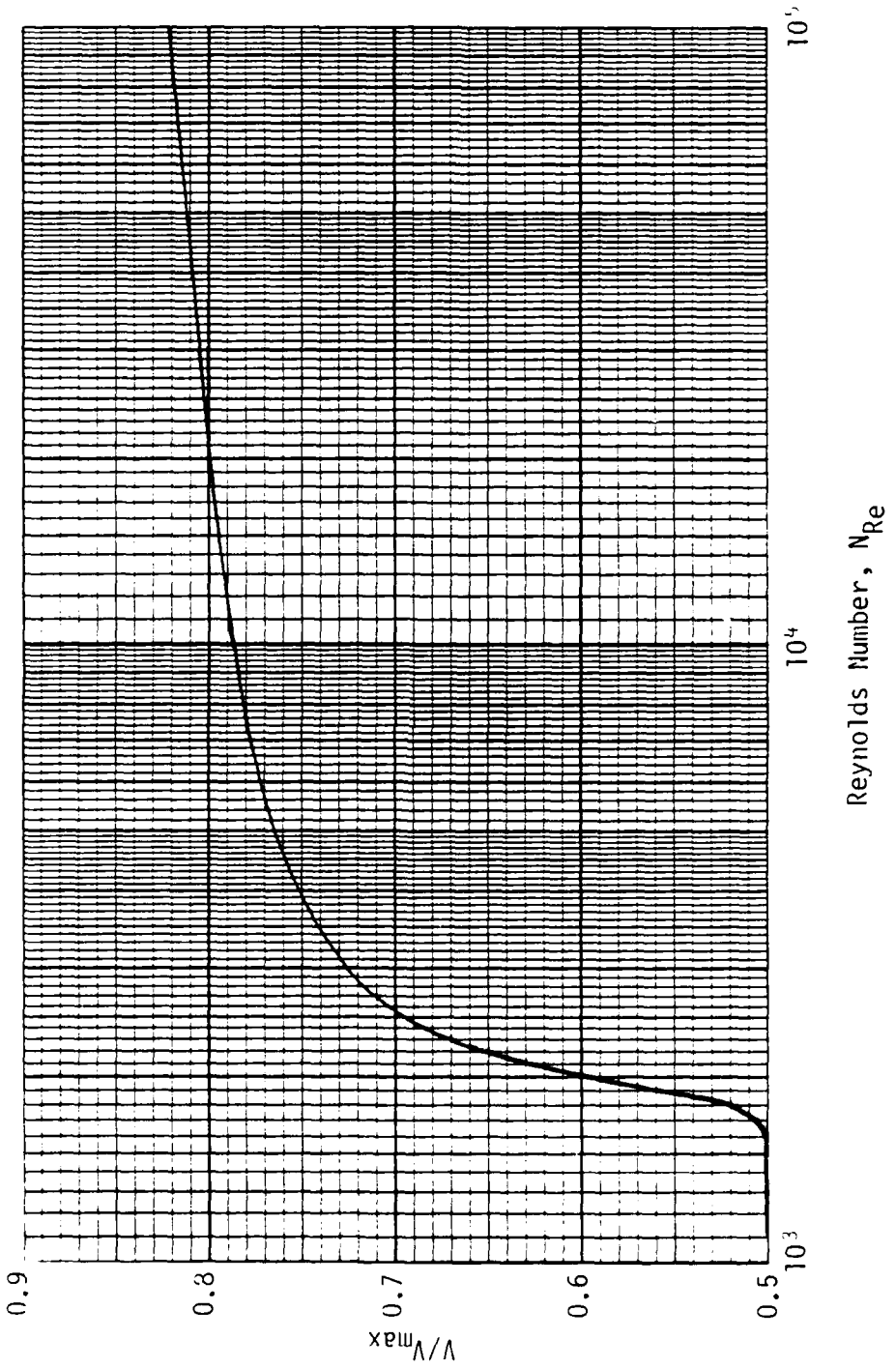

Figure 5-5. Average to Maximum Velocity V/V_{max} as a Function of Reynolds Number

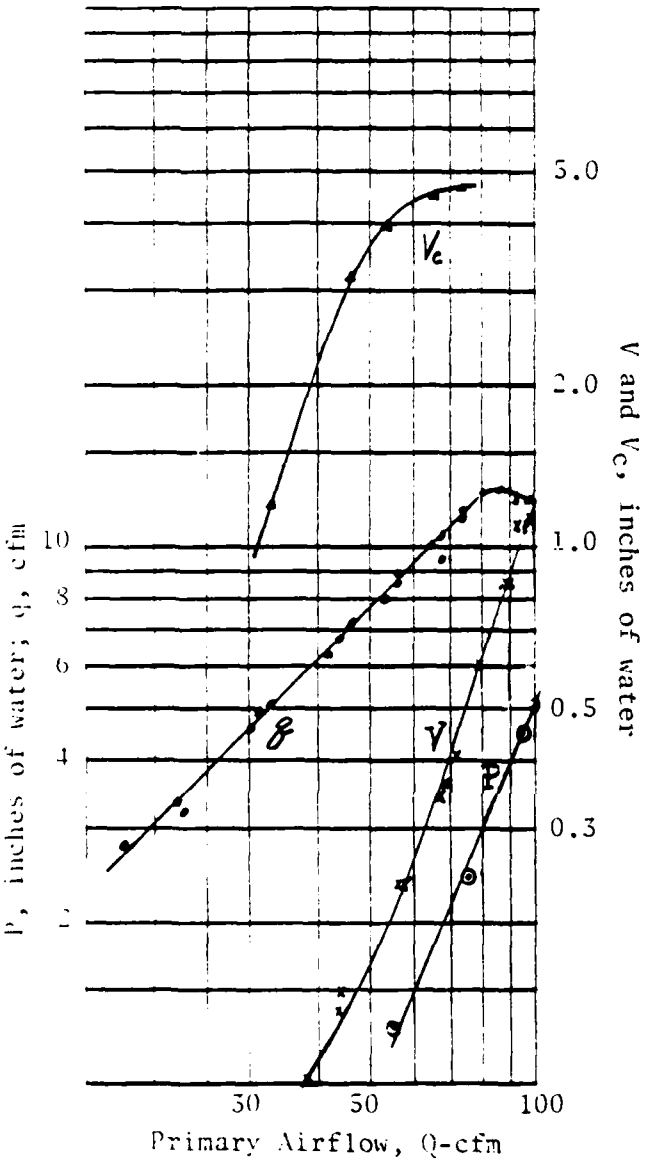

Figure 5-6. Secondary Flow q, Inlet Static Pressure P, and Induced Suction V and V_C, as a Function of Primary Flow Q, for Unit 1 Directly Coupled. V_C is Induced Suction With Inlet to Secondary Line Closed (q = 0).

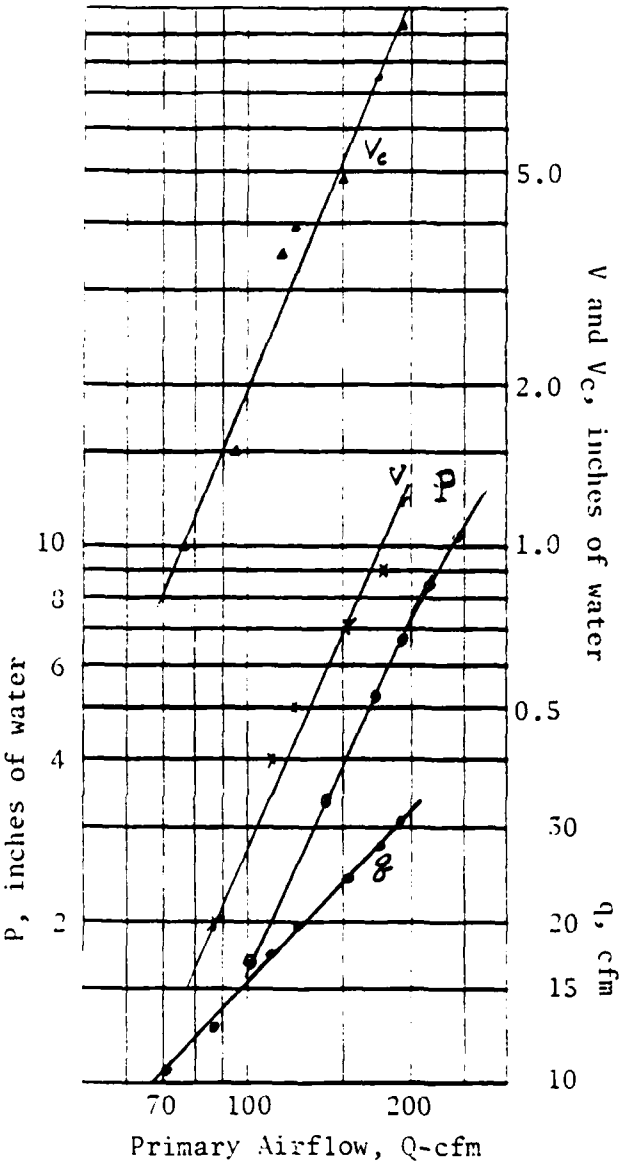

Figure 5-7. Secondary Flow q, Inlet Static Pressure, P, and Induced Suction V and V_C, as a Function of Primary Flow Q, for Unit 2 Directly Coupled. V_C is Induced Suction With Inlet to Secondary Line Closed (q = 0).

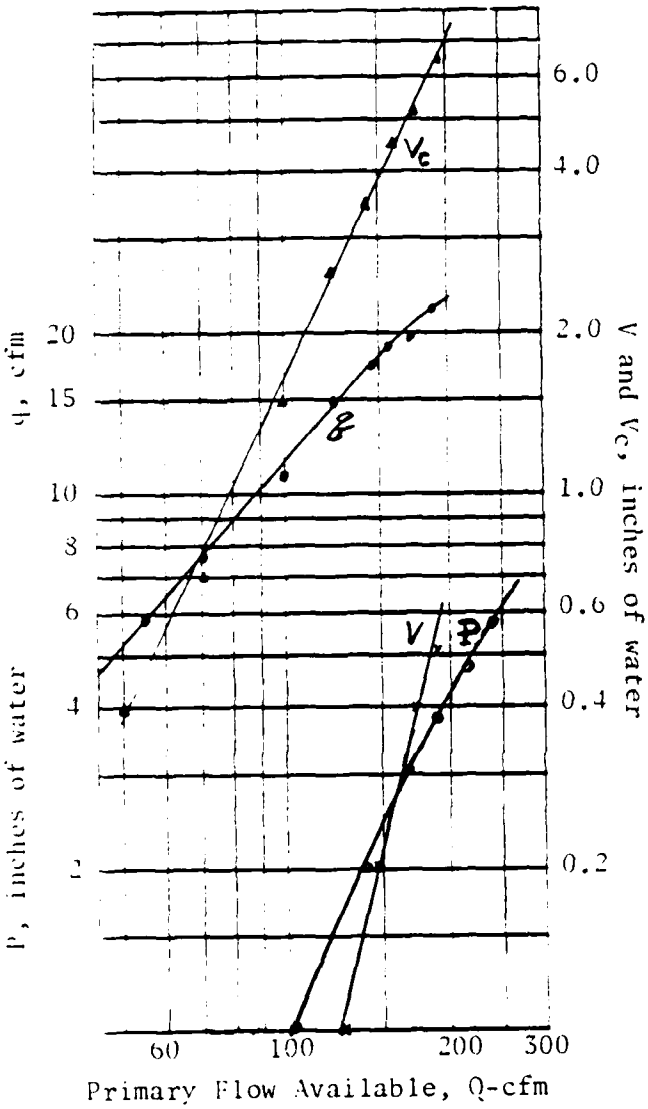

Figure 5-8. Secondary Flow q, Inlet Static Pressure P, and Induced Suction V and V_c as a Function of Primary Flow Q, for Unit 2 at 1-inch Separation. V_c is Induced Suction With Inlet to Secondary Line Closed (q = 0).

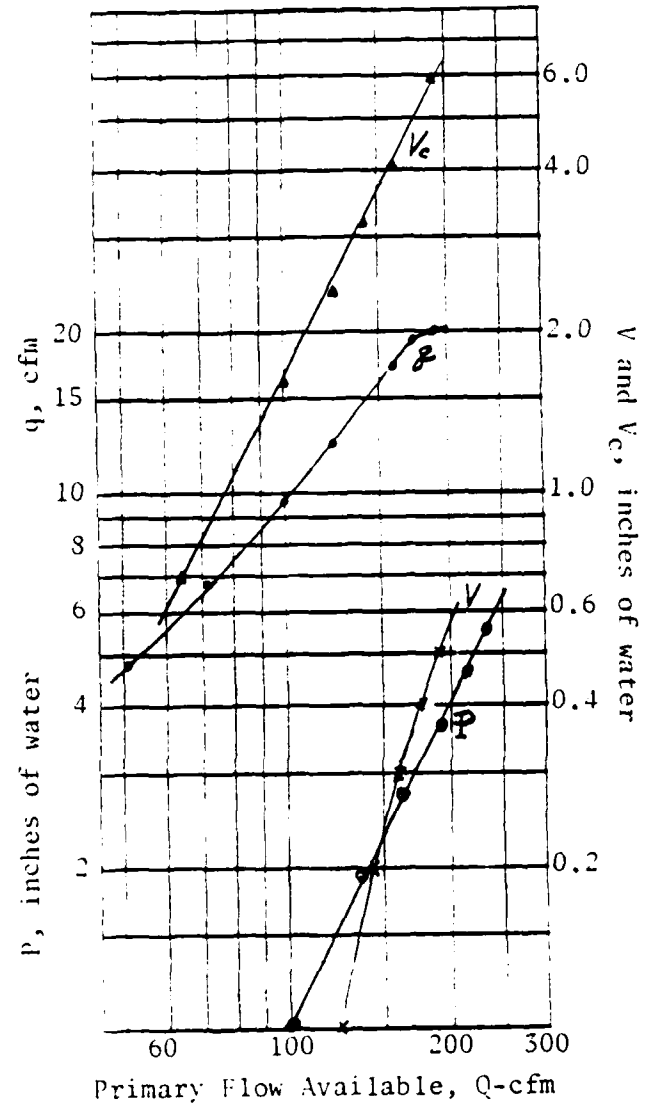

Figure 5-9. Secondary Flow q, Inlet Static Pressure and Induced Suction V and V_c as a Function of Primary Flow Q, for Unit 2 at 2-inch Separation. V_c is Induced Suction With Inlet to Secondary Line Closed (q = 0).

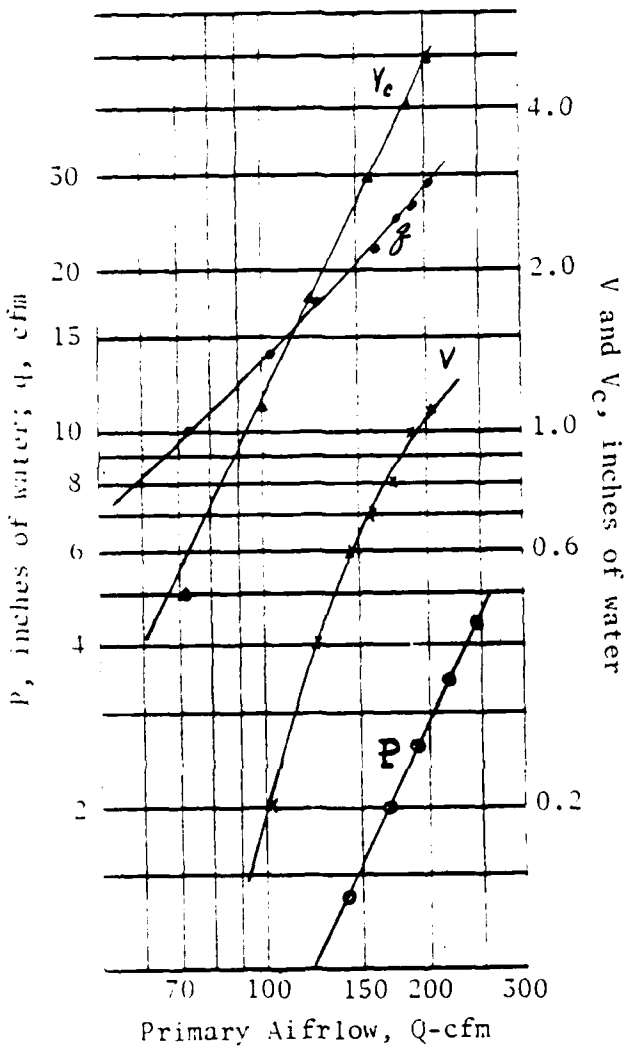

Figure 5-10. Secondary Flow q, Inlet Static Pressure P, and Induced Suction V and V_c, as a Function of Primary Flow Q, for Unit 3 Directly Coupled. V_c is Induced Suction with Inlet to Secondary Line Closed (q = 0).

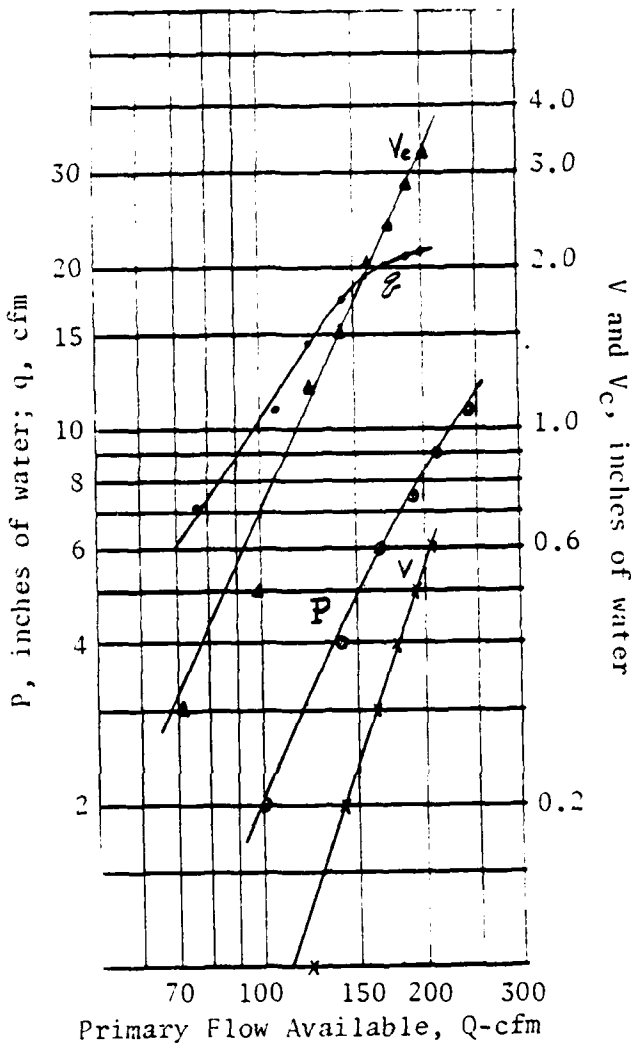

Figure 5-11. Secondary Flow q, Inlet Static Pressure P, and Induced Suction V and V_c, as a Function of Primary Flow Q, for Unit 3 at 1-inch Separation. V_c is Induced Suction With Inlet to Secondary Line Closed (q = 0).

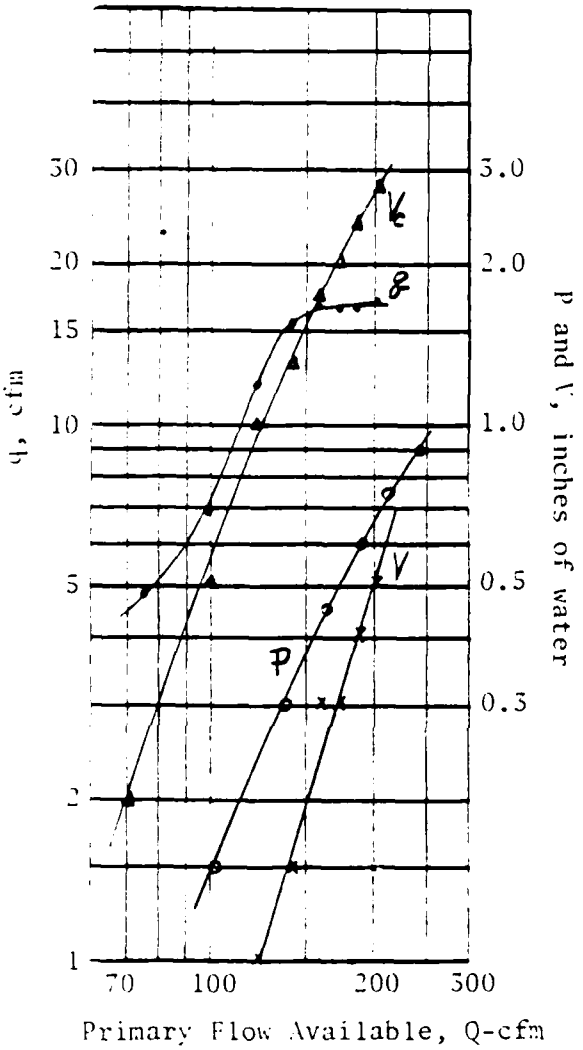

Figure 5-12. Secondary Flow q, Inlet Static Pressure P, and Induced Suction V and V_c, as a Function Primary Flow Q, for Unit 3 at 2-inch Separation. V_c is Induced Suction With Inlet to Secondary Line Closed (q = 0).

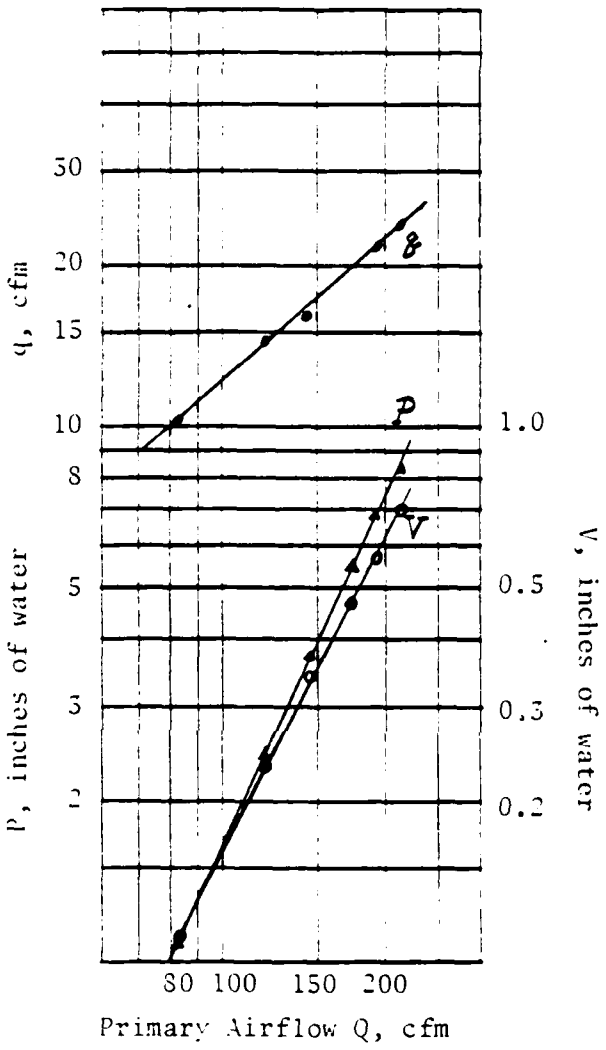

Figure 5-13. Secondary Flow q, Inlet Static Pressure P, and Induced Suction V as a Function of Primary Flow Q, for Unit 4.

Table 5-2. Characteristic Equations for Secondary Flow q as a Function of Primary Flow Q for x = 0,1 and 2 inches, z = 0

Unit	Equation	Range
2	$q_0 = .114Q^{1.061}$	$60 \leq Q \leq 200$
2	$q_1 = .076Q^{1.081}$	$50 \leq Q \leq 200$
2	$q_2 = .033Q^{1.234}$	$65 \leq Q \leq 180$
3	$q_0 = .107Q^{1.048}$	$60 \leq Q \leq 200$
3	$q_1 = .016Q^{1.396}$	$70 \leq Q \leq 160$
3	$q_2 = .000375Q^{2.142}$	$90 \leq Q \leq 145$
4	$q_0 = .214Q^{.830}$	$90 \leq Q \leq 220$

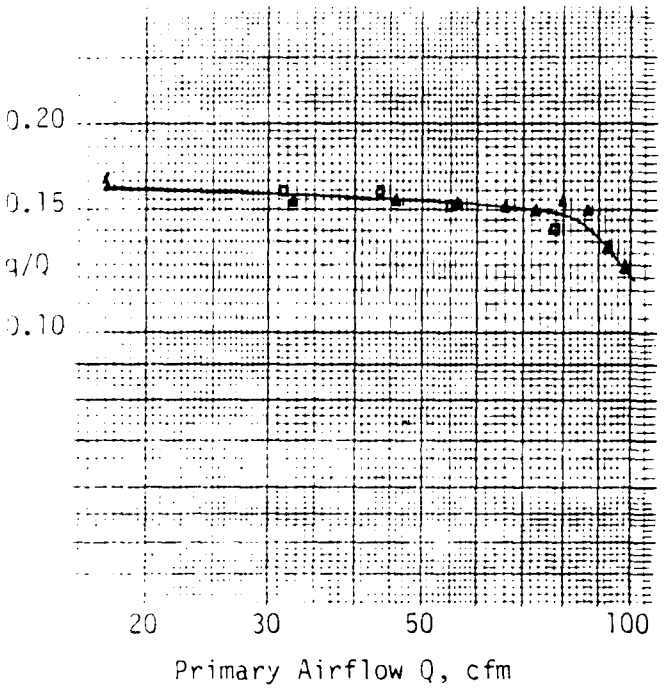

Figure 5-14. Ratio q/Q Vs. Q for Fan-Airpump No. 1, Directly Coupled on Centerline

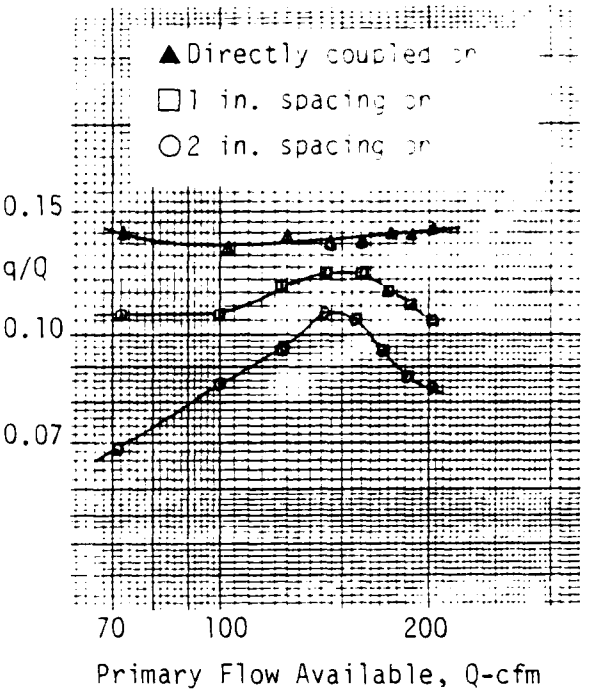

Figure 5-16. Ratio q/Q Vs. Q for Fan-Airpump No. 3

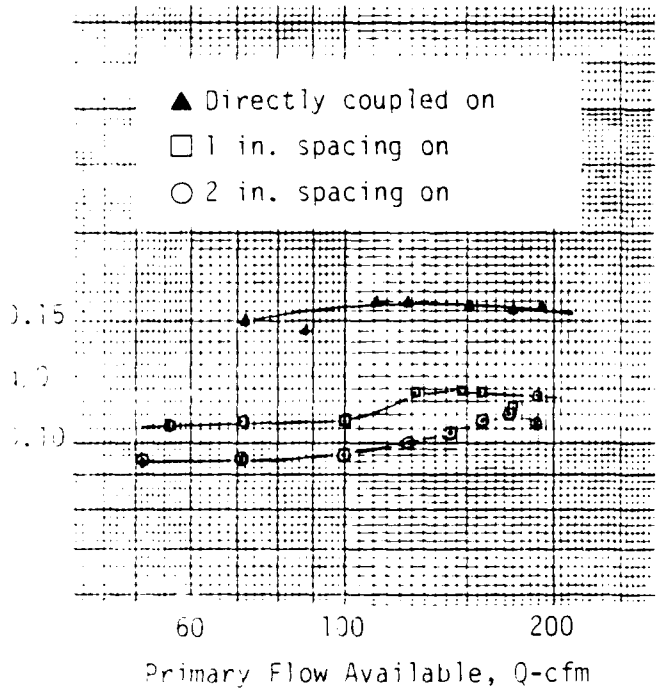

Figure 5-15. Ratio q/Q Vs. Q for Fan-Airpump No. 2

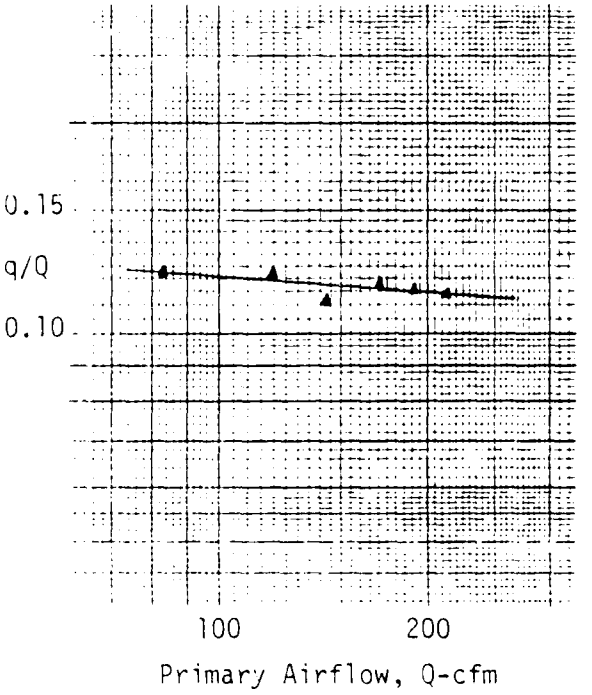

Figure 5-17. Ratio q/Q Vs. Q for Fan-Airpump No. 4, Directly Coupled On Centerline

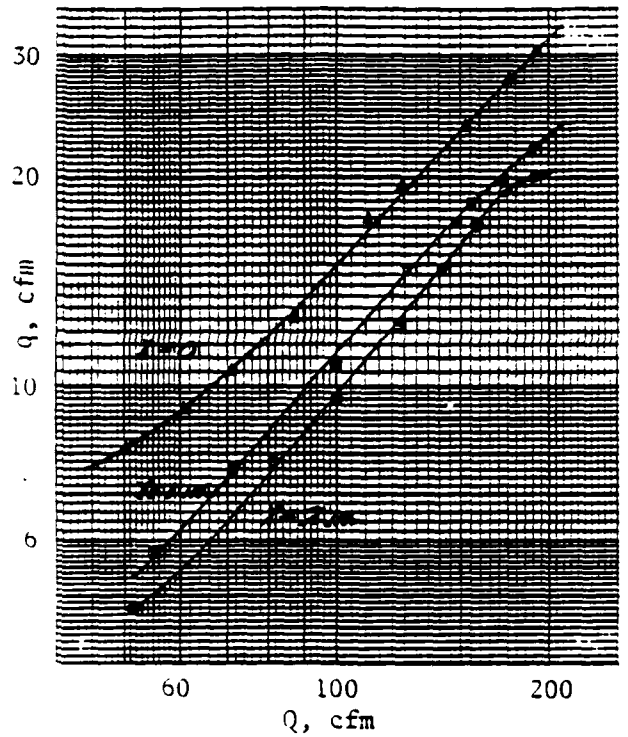

Figure 5-18. Secondary Flow q as a Function of the Available Primary Flow Q for x = 0,1 and 2 inches, Unit 2 on Centerline

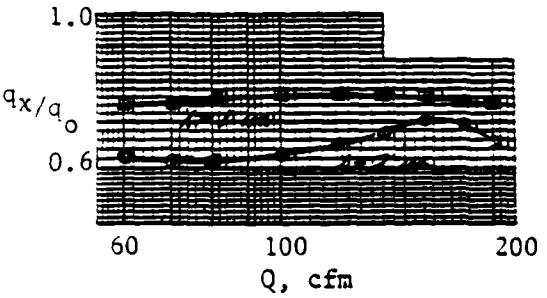

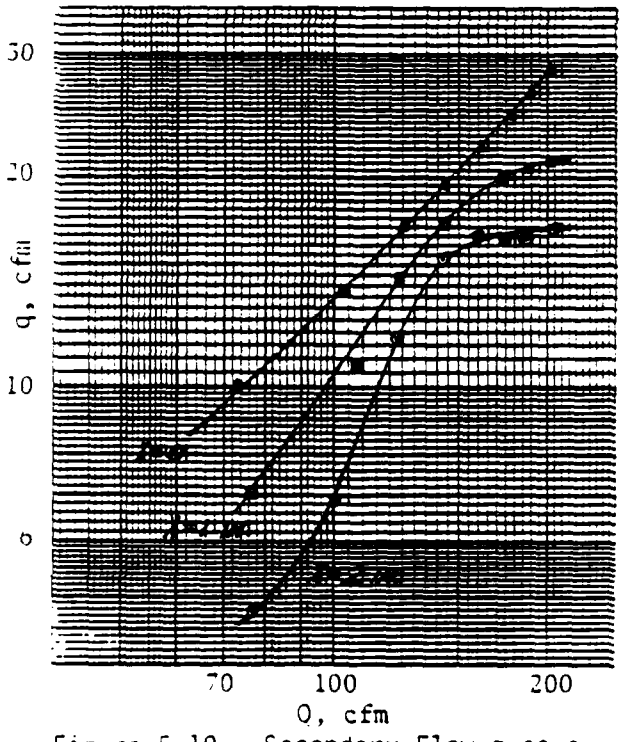

Figure 5-19. Secondary Flow q as a Function of the Available Primary Flow Q for x = 0,1 and 2 inches, Unit 3 on Centerline

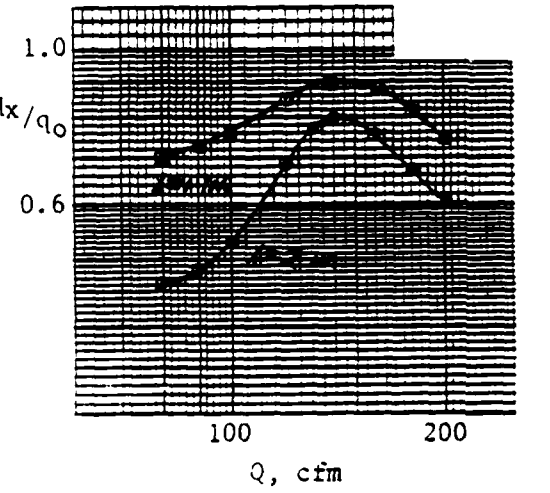

Figure 5-20. Ratio of Secondary Flow at X to Secondary Flow at X = 0 as a Function of Q, Units 2 and 3

Since the radius of the jet depends on its distance from the exit, as illustrated in Figure 5-21, velocity profiles can be calculated as a function of x. Figure 5-22 shows one half of the theoretical velocity profile for x equal to 1 and 2 inches, with r equal to the radii at the entrance to fan-airpumps 2 and 3. The profile is assumed to be symmetrical about the centerline.

Neglecting entrance effects, theoretical velocity values close to the wall are nearly zero. In the range for r/r_b from 1.0 to about 0.45, V/V_c rises steadily to 0.45-0.55, and thereafter increases more slowly as r/r_b is decreased. Since this profile concentrates flow in a region near the centerline, most of the available flow is expected to enter the bell. This, however, was not the case. Volumetric data for unit 2, based on continuity, showed that capture efficiency ranged from 71 to 77 percent at x = 1, the flow losses apparently being caused by resistance within the unit.

For practical purposes, it is more appropriate to deal with the average velocity $\overline{V}$, particularly when the data are to be correlated in terms of flow rate. Because of symmetry, the average velocity of the jet at the bell entrance can be calculated by summing up all velocities over the profile from r = 0 to r = r_b and dividing by the bell radius, r_b:

$$\overline{V} = \frac{1}{r_b} \int_0^{r_b} V_c 10^{-.3(r/r')^2} r dr \tag{4}$$

When this is done, $\overline{V}/V_c$ for unit 2 (in this series of tests) becomes 0.45 and 0.37 at x = 1 and 2 inches, respectively. For unit 3, these values become 0.56 and 0.47. The theoretical flow rate is the product of the cross-sectional area and the average velocity. Actual values for flow must consider capture efficiency as discussed above.

Using these velocity ratios and appropriate values for capture efficiency, it is possible to correlate the secondary flow data for unit 2. In the range $60 \leq Q \leq 190$ cfm, q_0 and q_1 can be correlated within 5 percent by:

$$q_0 = 0.114Q^{1.061} \tag{5}$$

$$q_1 = 0.076Q^{1.081} \tag{6}$$

where q_0 and q_1 are the secondary flows for 0- and 1-inch separation respectively. Since the ratio of q_1/q_0 is proportional to the capture efficiency, Γ becomes:

$$\Gamma = (k_1/k_0)Q^{C_1 - C_0} = 0.670Q^{0.02} \tag{7}$$

which gives $0.727 \leq \Gamma \leq 0.744$ for $60 \leq Q \leq 190$. This is in good agreement with the average measured value for Γ of 0.74, for $180 \leq Q \leq 225$.

The data for q_2 and q_1 can also be correlated by analyzing mainstream velocities. Since the inlet areas are equal, the ratio q_2/q_1 as a function of Q is proportional to the ratio of the average mainstream velocities:

$$q_2/q_1 = \overline{V}_2/\overline{V}_1 = .45V_0/.37V_0 = 0.82 \tag{8}$$

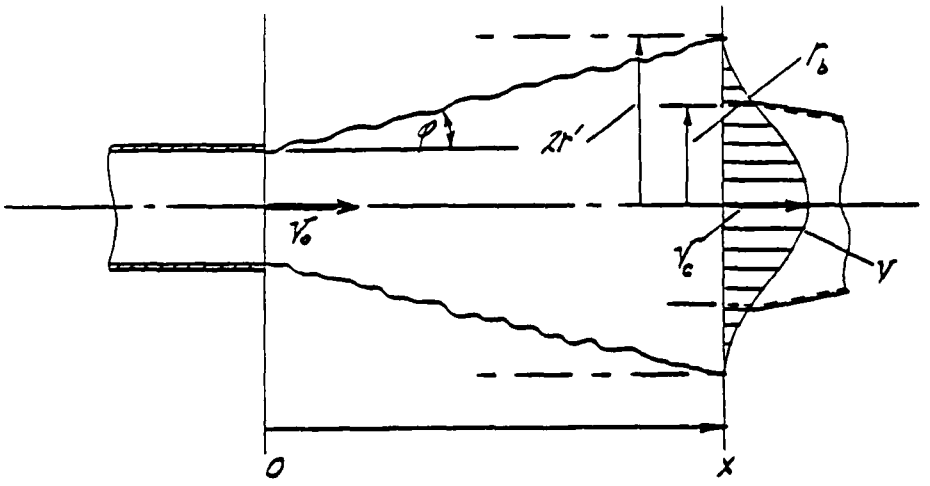

Figure 5-21. Expansion of Free Jet from Source to Fan-Airpump Entrance

		x=1		x=2	
Unit	r_b	r/r'	r'	r/r'	r'
2	1.38	0≤2.23	.62	0≤1.94	.71
3	1.75	0≤2.82	.62	0≤2.46	.71

	Unit 2	Unit 3
X	$\bar{V}/V_c$	$\bar{V}/V_c$
1	0.45	0.56
2	0.37	0.47

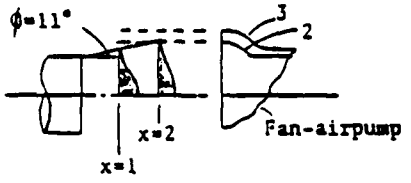

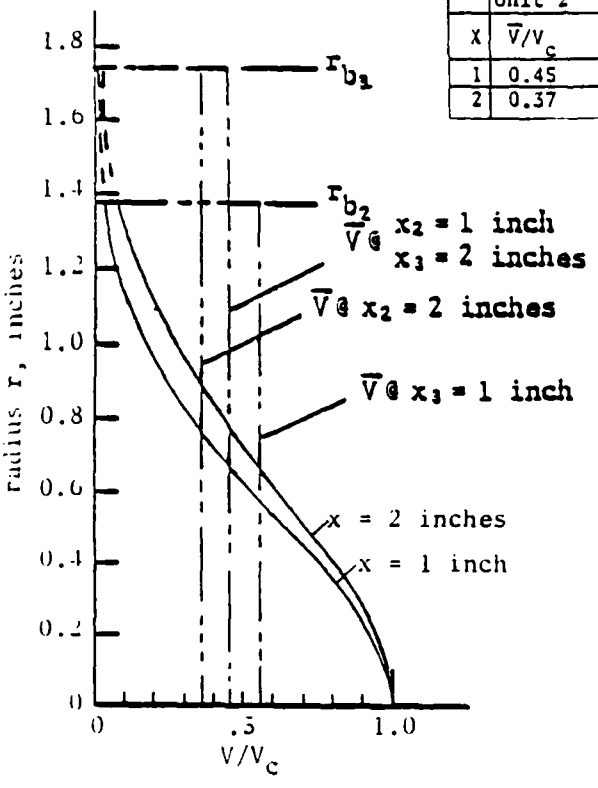

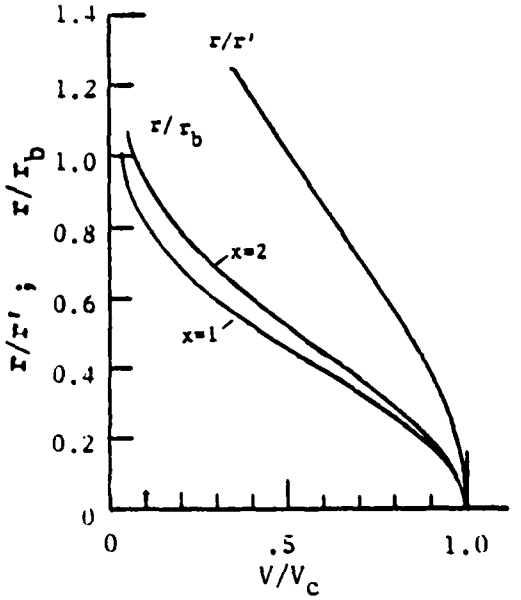

Figure 5-22. Velocity Distribution in Free Jet from Circular Orifice

For the range $60 \leq Q \leq 175$, above which q_2 remains relatively constant for increasing Q, the ratio q_1/q_2 can also be written in terms of the characteristic flow equations:

$$q_2/q_1 = 0.033Q^{1.234}/0.076Q^{1.081} = 0.437Q^{0.153} \quad (9)$$

This gives $0.818 \leq q_2/q_1 \leq 0.963$ for $60 \leq Q \leq 175$. Data for q_2/q_1, calculated from average velocity values and from the characteristic equations, are given in Figure 5-23, along with the experimental results. These curves show good correlation between the experimental and theoretical data. This is significant because it provides a meaningful way to analyze the airflow environment within the engine compartment. By mapping the rate and direction of the flows being developed by the radiator fan, induced airflow can be predicted for various fan-airpump placements and sizes. On-vehicle data are presented and discussed later in the report.

5.2.3. **Nonconcentric Alignment.** Another parameter that must be considered is fan-airpump orientation with respect to the direction of the mainstream flow. This parameter was investigated in the laboratory by repeating the previous series of tests for units 2 and 3, but with angular displacements for α of 35 and 60 degrees, as shown in Figure 5-24. Results for these tests are shown in Figures 5-25 through 5-30.

The curves in Figure 5-25 show results for four combinations of α and **x**, for $\beta >$ and $< 90^{\circ}$. There is a significant difference in secondary flow development depending on whether the primary flow is directed toward or away from the secondary flow port (that is, whether $\beta >$ or $< 90^{\circ}$ in Figure 5-23). The extent of this difference increases with increasing values of α and **x**. For $\alpha = 60^{\circ}$ and **x** = 2 inches, secondary flow cannot be maintained over the normal range of Q when $\beta = 30$. For $\beta > 90^{\circ}$, secondary flow is decreased, but well-behaved over the entire range of interest.

Figure 5-26 shows secondary flow development as a function of α at **x** = 1, for $\beta >$ and $< 90^{\circ}$. As can be seen, the effect of angular displacement on secondary flow development is substantially less for $\beta > 90^{\circ}$ than for $< 90^{\circ}$. A similar effect is shown in Figure 5-27 for unit 3, where **q/Q** is plotted versus Q. The affect of separation distance on secondary flow development is also less for $\beta > 90$, as shown in Figure 5-27 and Figure 5-28. These findings are of practical importance. Apparently the fan-airpump is much more tolerant of primary airflow aberations if the secondary flow duct is properly oriented to the flow ($\beta > 90^{\circ}$). Figure 5-29 shows an interesting correlation of the data. There is a close parallel in secondary flow development for $\alpha = 35^{\circ}$ at 2-inch separation and $\alpha = 60^{\circ}$ at 1-inch separation. However, there is a significant difference in these sets of data depending on whether β is $>$ or $< 90^{\circ}$.

The relative impact of separation distance and orientation on secondary flow development is shown in Figure 5-30 for unit 2. These curves, with the exception of curve 11, are based on the characteristic equations developed earlier. The trend is rather explicit. As expected, secondary flow decreases with increasing separation and angular divergence. The flow for $\alpha = 60^{\circ}$ and **x** = 2 inches

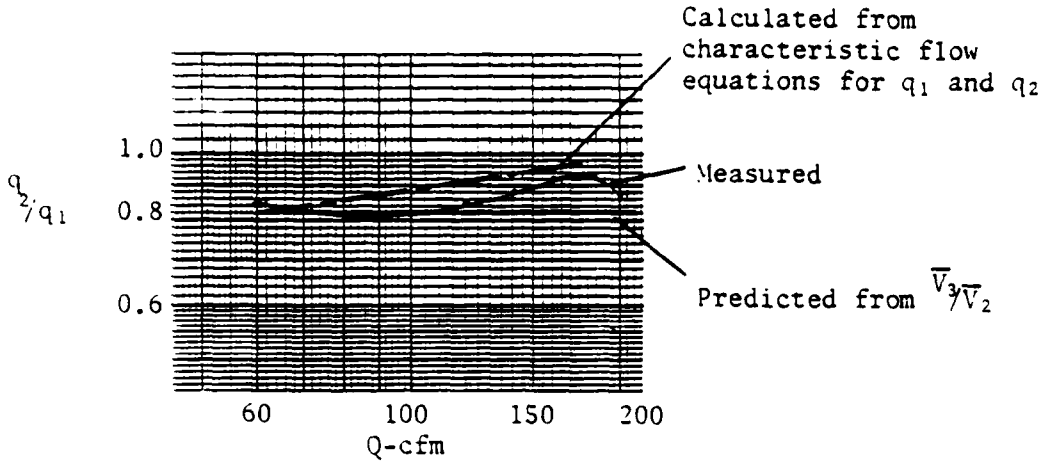

Figure 5-23. The Ratio q_2/q_1 as a Function of Primary Available Flow Q for Unit 2 at α = 0 (q_1 is q at x = 1 inch, q_2 is q at x = 2 inches)

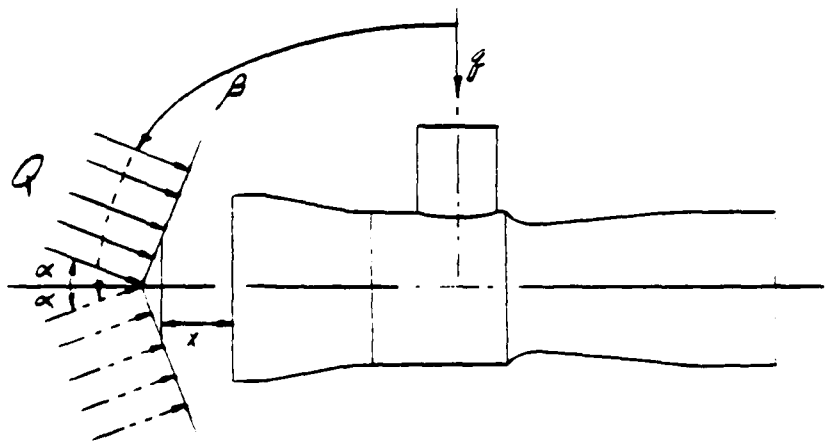

Figure 5-24. Test Arrangement for Investigating Fan-Airpump Performance as a Function of Orientation With Respect to the Direction of the Primary Flow, Q. α Was Set at 35° and 60° on Both Sides of the Centerline, Therefore, β Ranged From 30° to 150°. X was Set at 1 and 2 Inches.

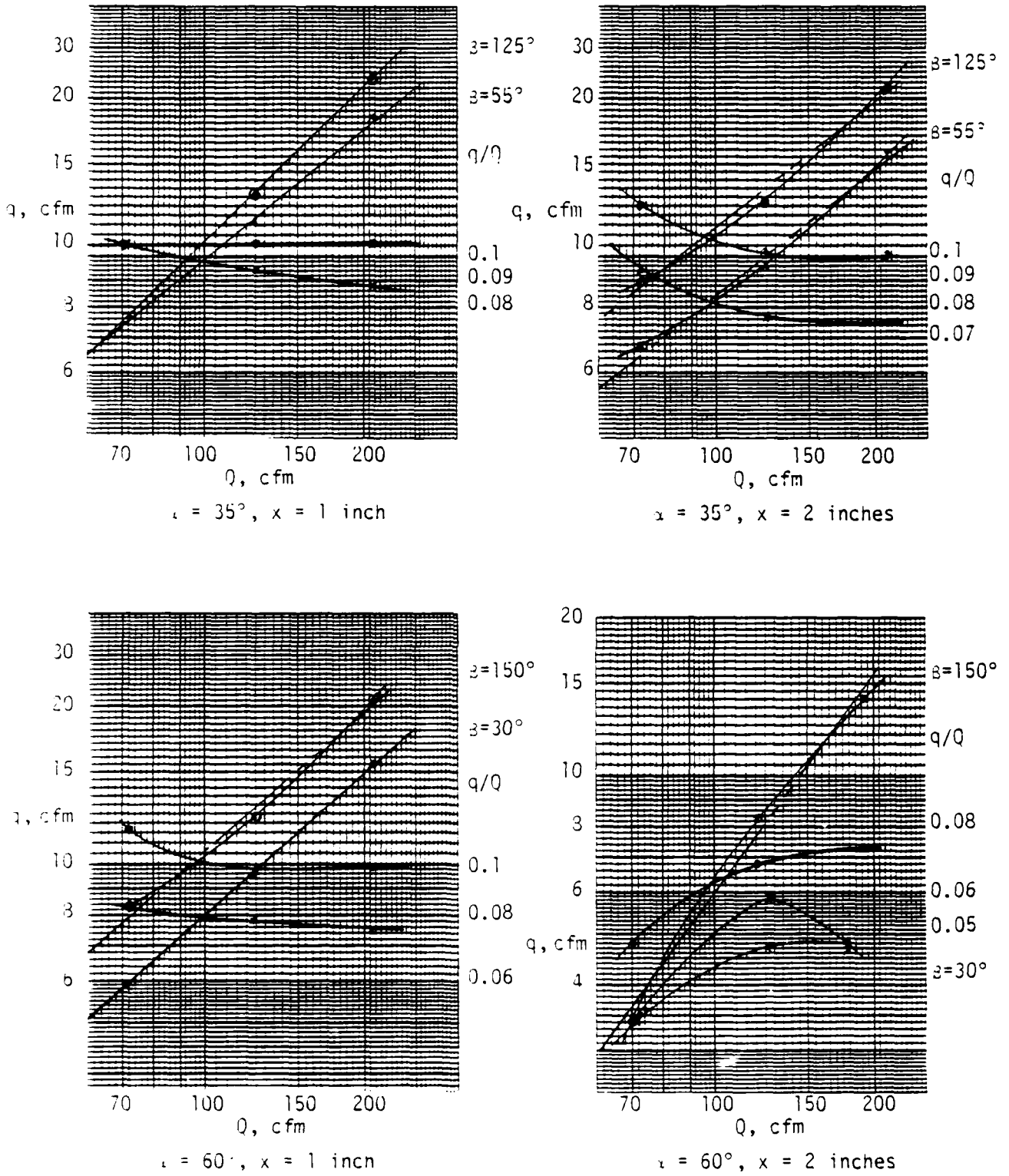

Figure 5-25. Secondary Airflow Data as a Function of Q and β for α = 35° and 60°, x = 1 and 2 inches (Unit 2)

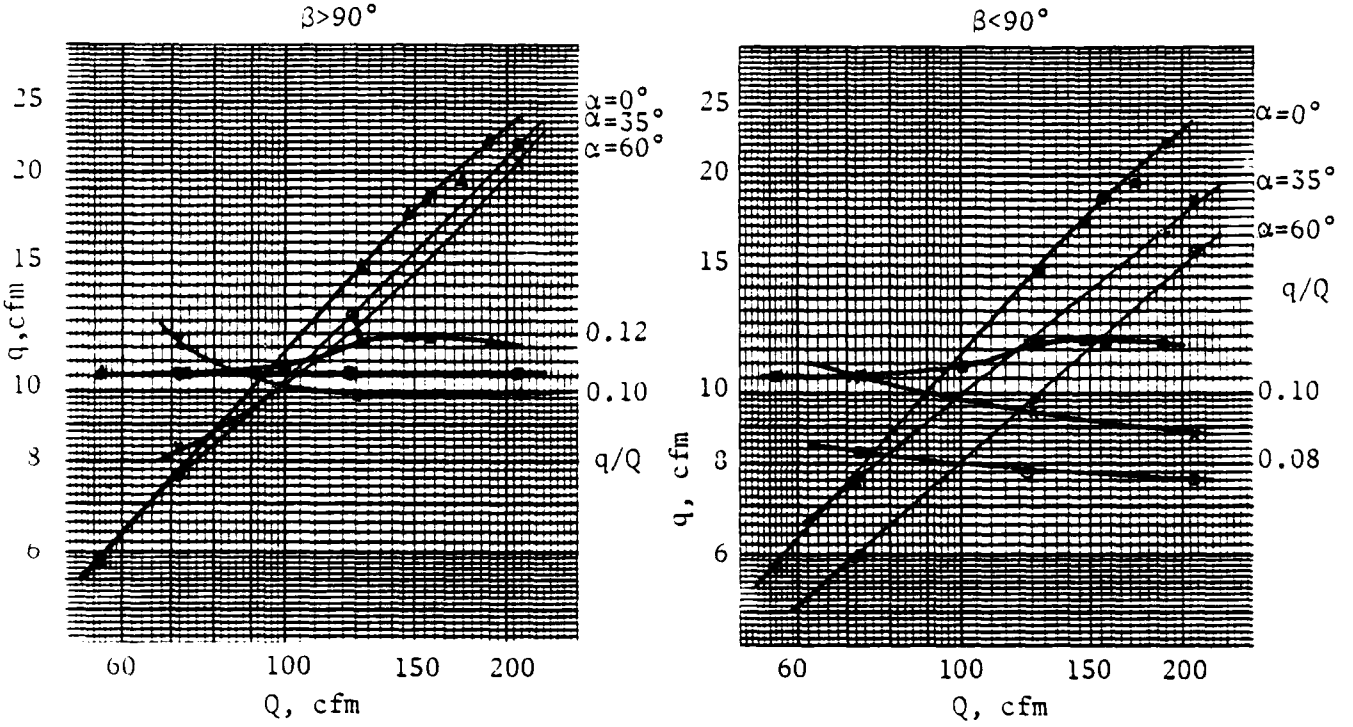

Figure 5-26. Impact of α on Secondary Flow Development at x = 1 inch for β > and < 90° (Unit 2)

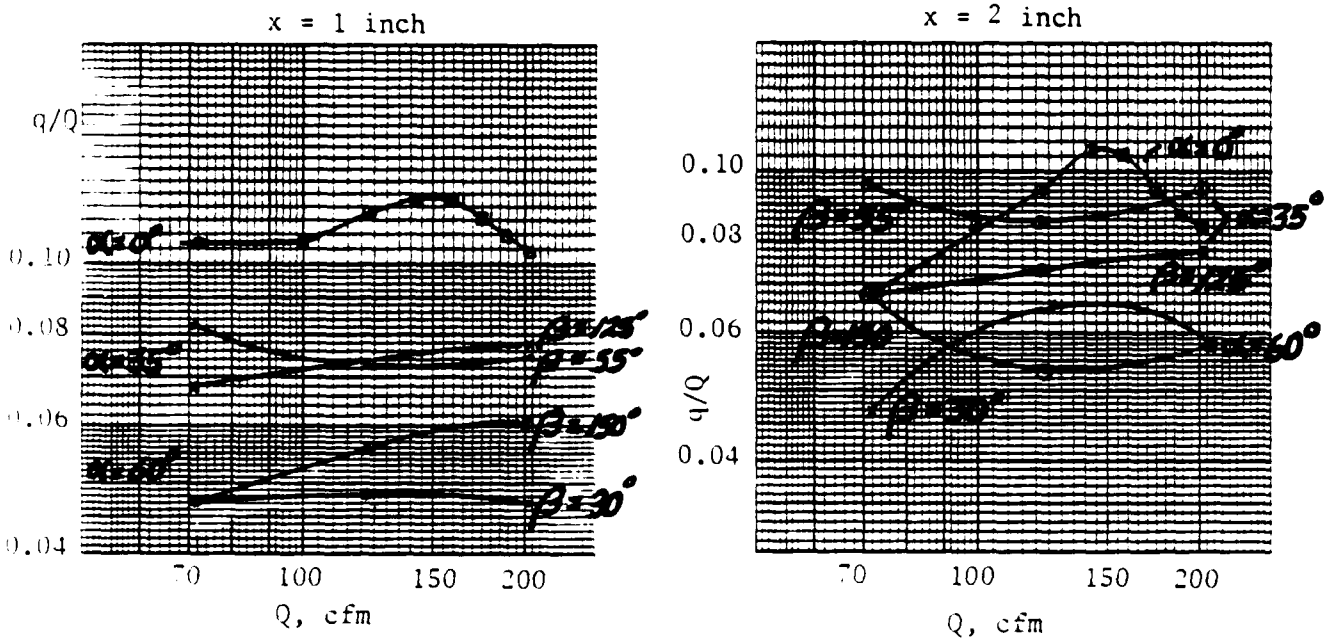

Figure 5-27. q/Q Versus Q for Unit 3 at 1- and 2-inch Separation for α = 0, 35, and 60° (β > and < 90°)

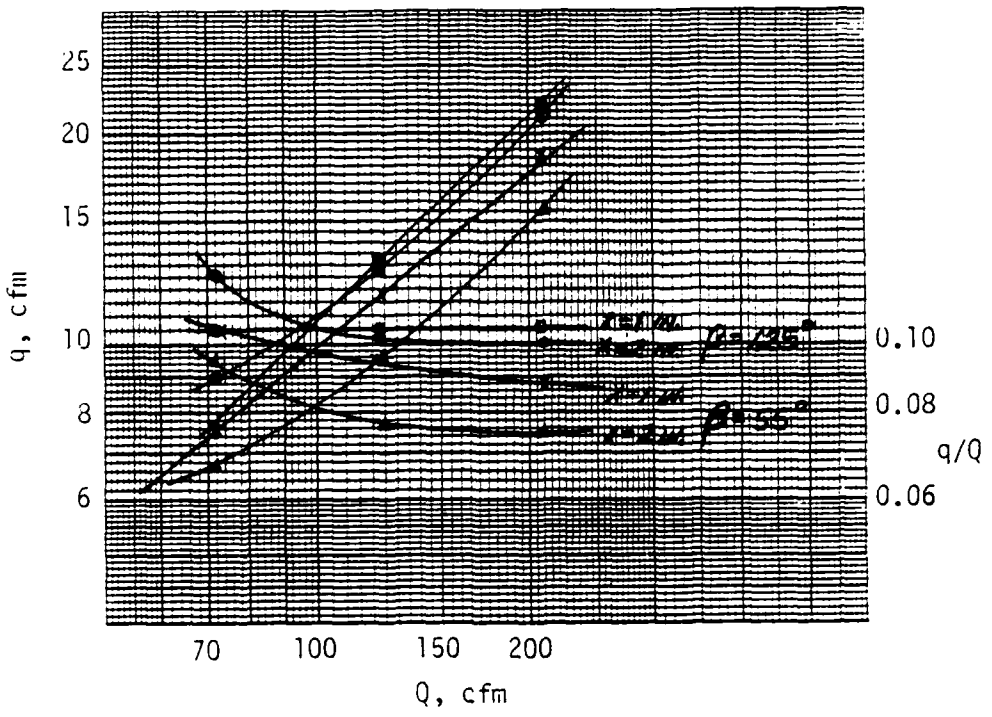

Figure 5-28. Impact of Separation Distance and β on Secondary Flow Development, α = 35° (Unit 2)

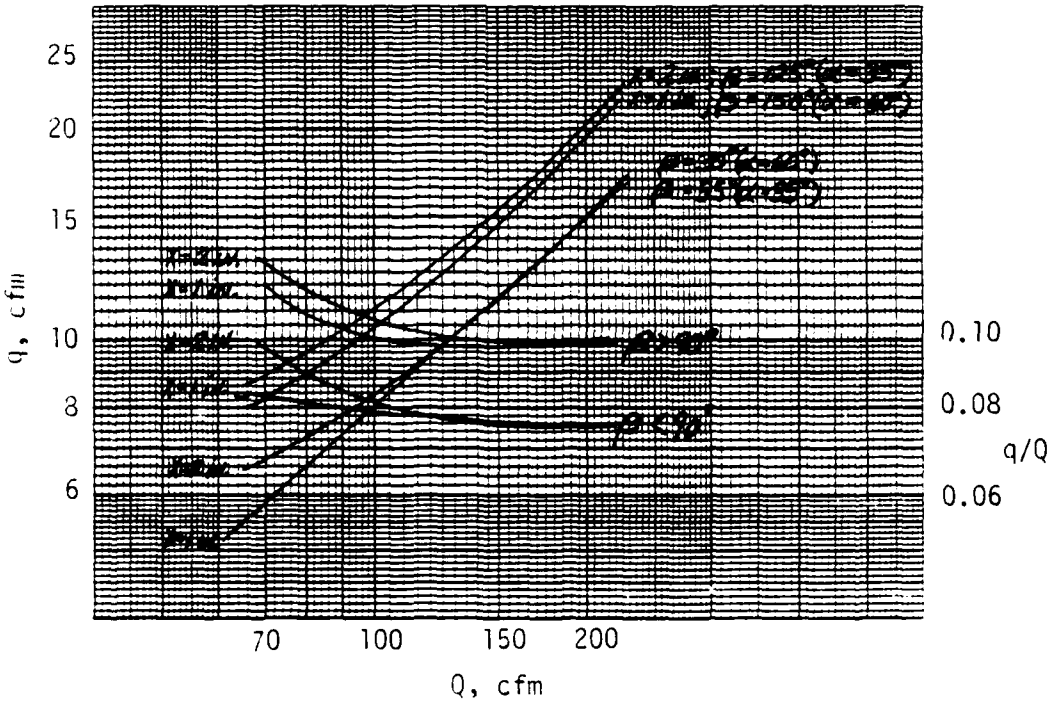

Figure 5-29. Comparison of Secondary Flow Data for α = 35° at 2 inches and α = 60° at 1 inch (Unit 2)

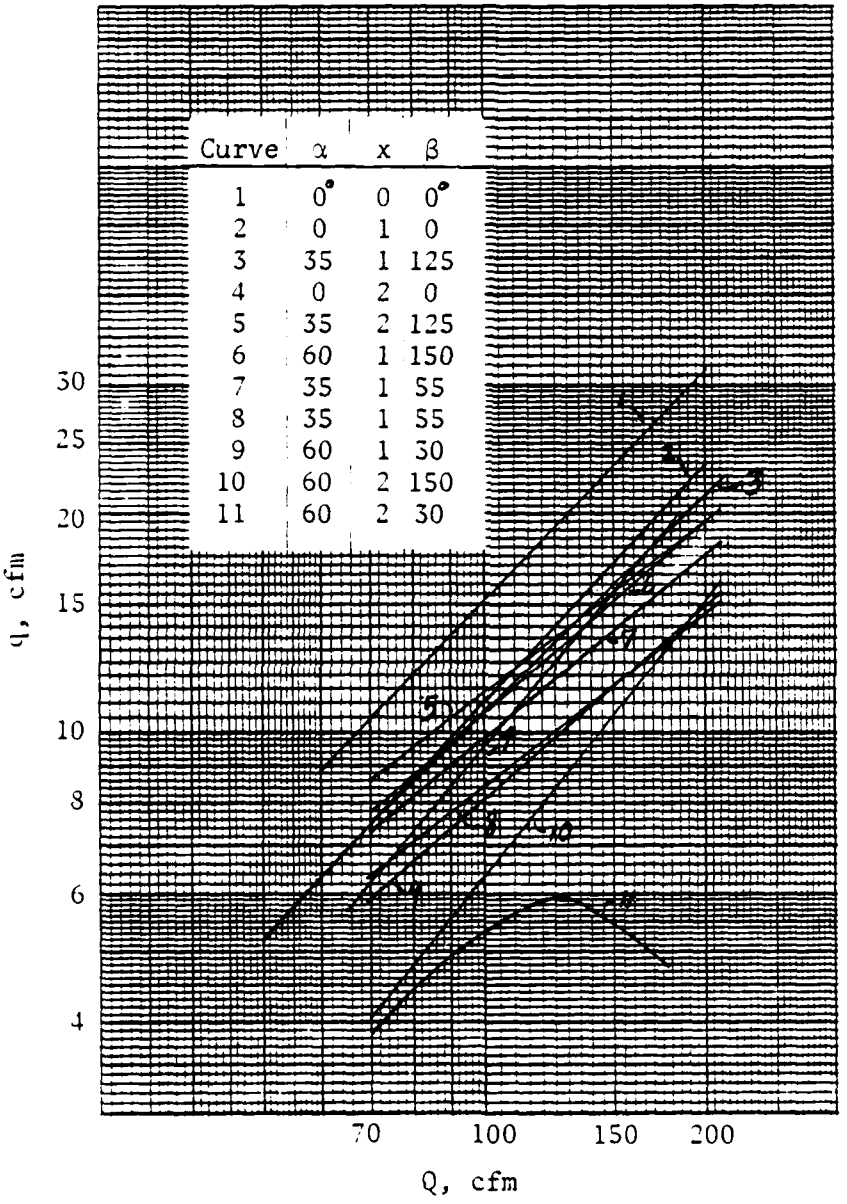

Figure 5-30. Secondary Flow Development as a Function of Q for Given Values of α, x and β (Unit 2)

($\beta = 150^o$) is less than 50 percent of that for the centerline case ($\alpha = 0$, $x = 0$). What was not expected, however, was the impact on flow caused by β, the angular divergence measured with respect to the direction of the secondary flow tube. For small values of β, it appears that secondary flow development is limited. Curve 11 shows that **q** goes through a maximum and then declines as Q increases. The fact that curves 2-6 are relatively bunched together also indicates that secondary flow development is less critically affected by α and **x** when $\beta > 90^o$.

5.2.4. **On-Vehicle Airflow.** Airflow patterns developed by the radiator fan were measured on 2½- and 5-ton trucks. These measurements were made using a centerline pitot tube positioned inside a 2 7/8-inch inside diameter tube, the data being corrected as a function of Reynolds number to give average velocity values for calculating airflow. Mapping was accomplished by changing the position and orientation of the tube until the maximum velocity profile was obtained for a given area. By investigating several areas, an optimum location, with respect to airflow, was determined. Results are shown in Figures 5-31 and 5-32 where Q is plotted as a function of engine RPM. Secondary airflows, which were measured by placing the fan-airpumps at the same location and with the same orientation as the primary flow tube, are also given. These data, for unit 2, are combined in Figure 5-33 to indicate the difference in response between the two vehicles. For the 5-ton truck, the ratio **q/Q** was about 0.08. On the 2½-ton truck, the ratio was about 0.05, increasing to 0.07 when the inlet diameter was increased, ($d_{2A}/d_2 = 1.45$). As a means of comparison, **q/Q** for unit 3 on the 2½-ton truck was slightly greater than 0.10.

To compare the laboratory and on-vehicle data, the on-vehicle flow data are replotted in Figure 5-34 as a function of Q. This change in abscissa (from RPM to Q) makes it possible to estimate the laboratory case which best simulates a particular on-vehicle situation. The curves in Figure 5-34 confirm our previous conclusions, namely that secondary flow development is greater for the 5-ton truck than for the 2½-ton truck, and that flow development is improved when the larger entrance is used.

Figure 5-35 shows the on-vehicle data with selected laboratory data. The laboratory data shown were chosen because they match fairly well with the on-vehicle data and can therefore be used to imply the laboratory case which best simulates the on-vehicle situation. For the 2½-ton truck, the on-vehicle data for unit 3 are reasonably represented by the laboratory case where $\alpha = 0$ and $x = 1$ to 2 inches. In a similar manner, the data for unit 2 on the 5-ton truck match well for $\alpha = 35^o$ ($\beta = 55^o$) and $x = 1$ inch. This is confirmed in Figure 5-36, where laboratory data for **q/Q** are superimposed on the on-vehicle data. Because the 5-ton truck was best represented by the case where $\alpha \neq 0$, orientation on this vehicle was not optimized. The laboratory data indicate that a 30 percent improvement may be possible.

It is also interesting to note the on-vehicle data for unit 1. Here secondary flow is developed over a range of Q that extends far beyond the range indicated in Figure 5-6. It is difficult to compare these data, however, because the laboratory data were only developed for the directly coupled case, which indicates that **q** decreases, or is at best stabilized, for Q > 100 cfm. The on-vehicle data suggest

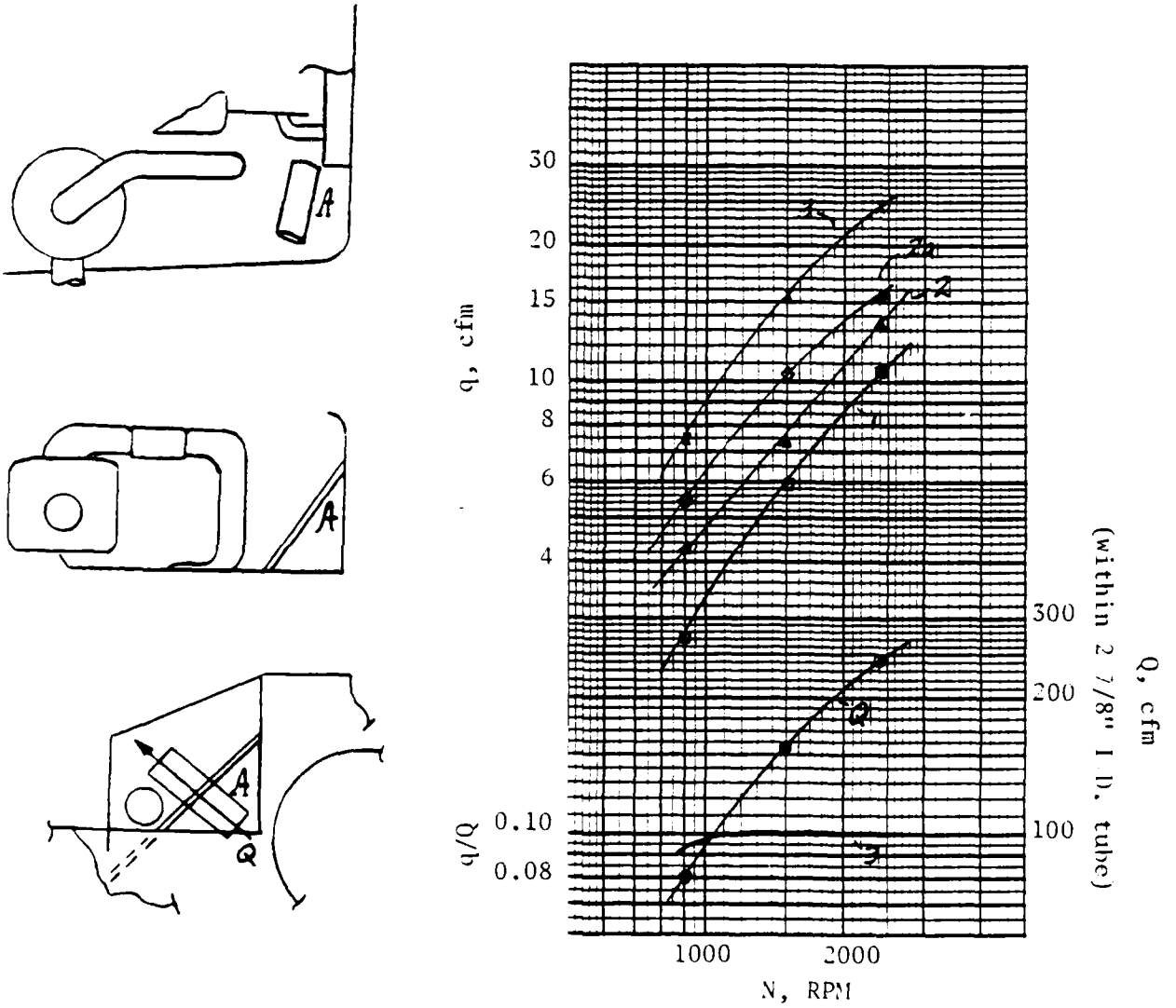

Figure 5-31. Flow Data as a Function of Engine Speed for 2-1/2-ton Truck. Measurements Made with Engine Compartment Open.

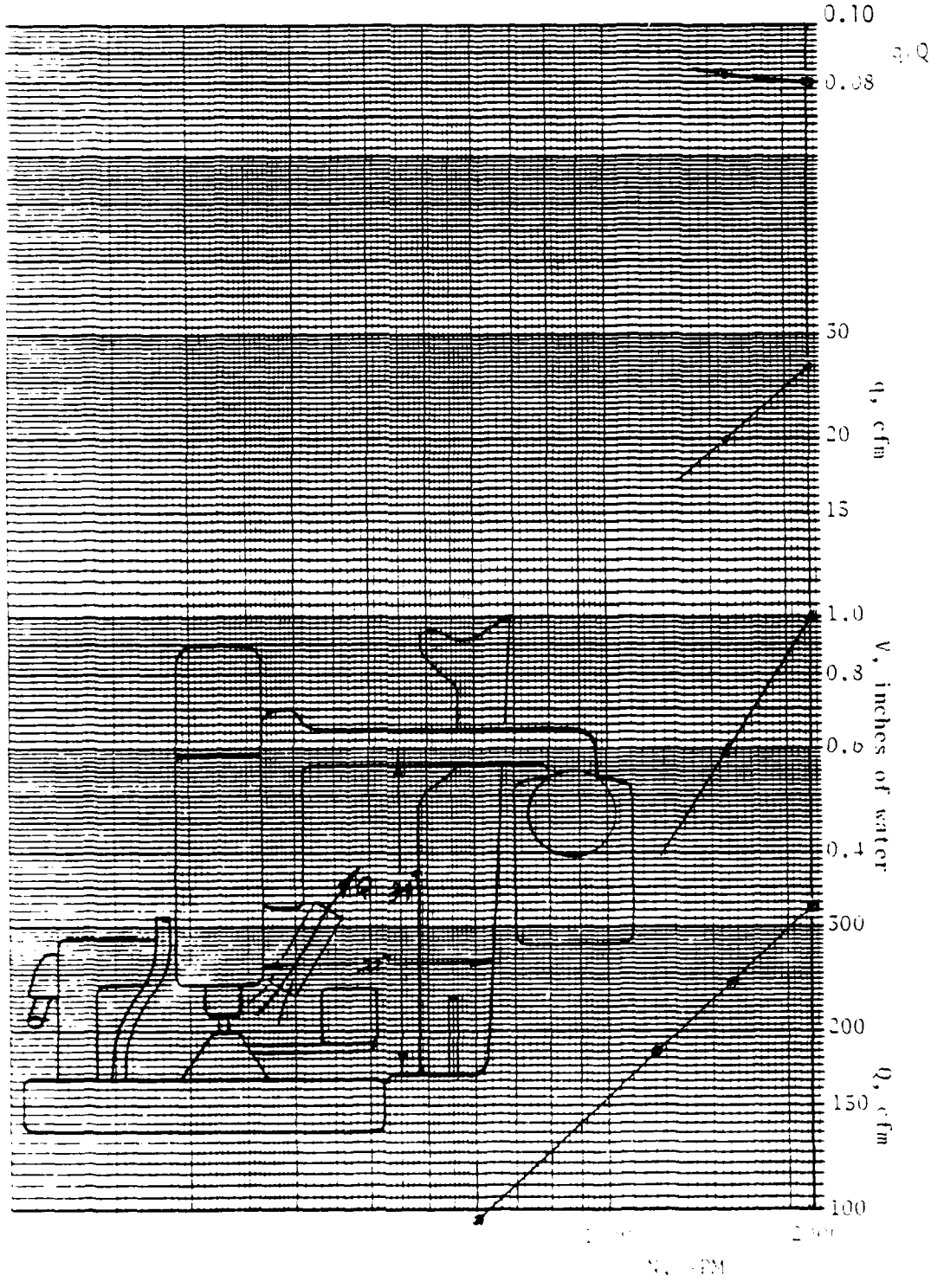

Figure 6-32. q/Q, Secondary Airflow q, Induced Suction V, and Primary Flow Q in 2-7/8 in. tube as a Function of Engine Speed for Unit 2 on 6-ton Truck. Measurements Made With Engine Compartment Open.

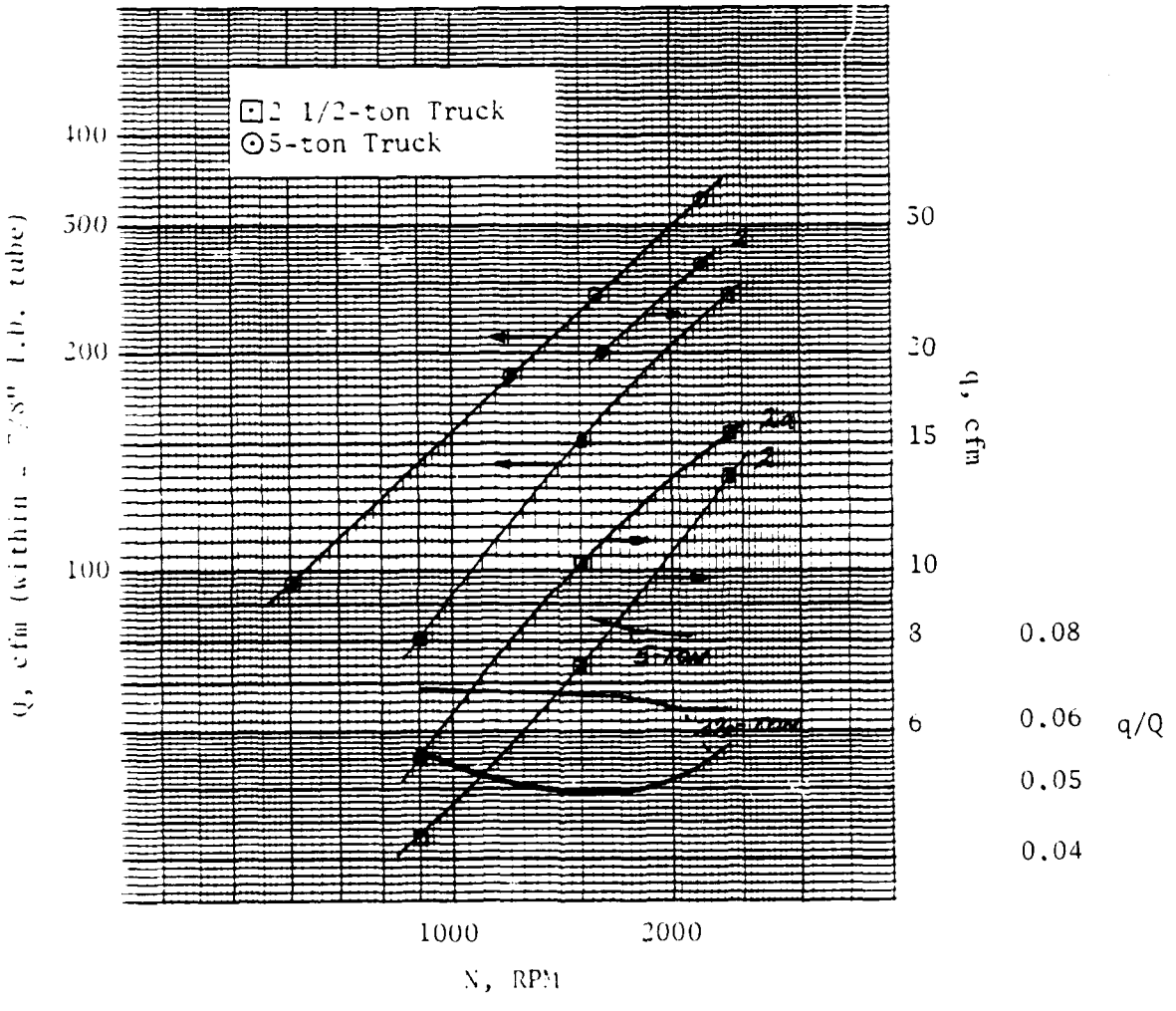

Figure 5-33. Airflow Data as a Function of Engine Speed for Units 2 and 2a on 2-1/2- and 5-ton Truck. Measurements Made With Engine Compartment Open.

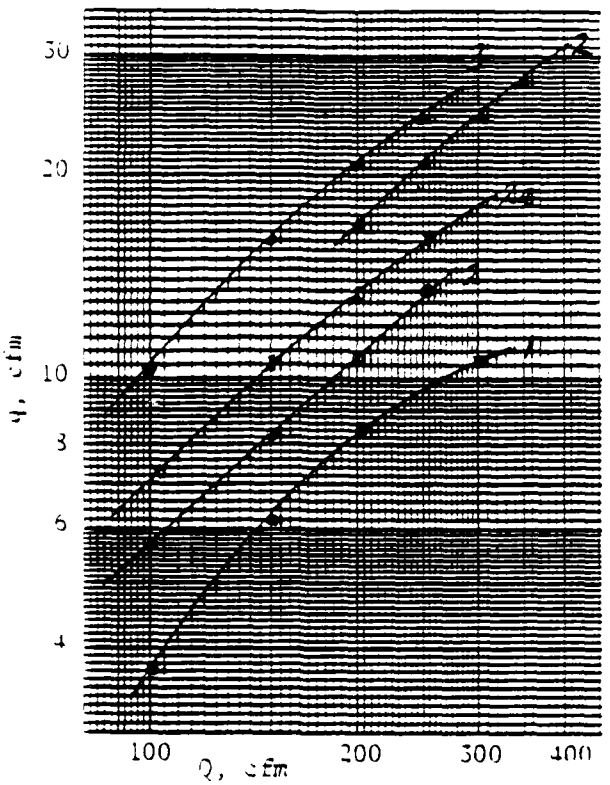

Figure 5-34. Secondary Flow q as a Function of Q for 2-1/2- and 5-ton Truck. Measurements Made With Engine Compartment Open.

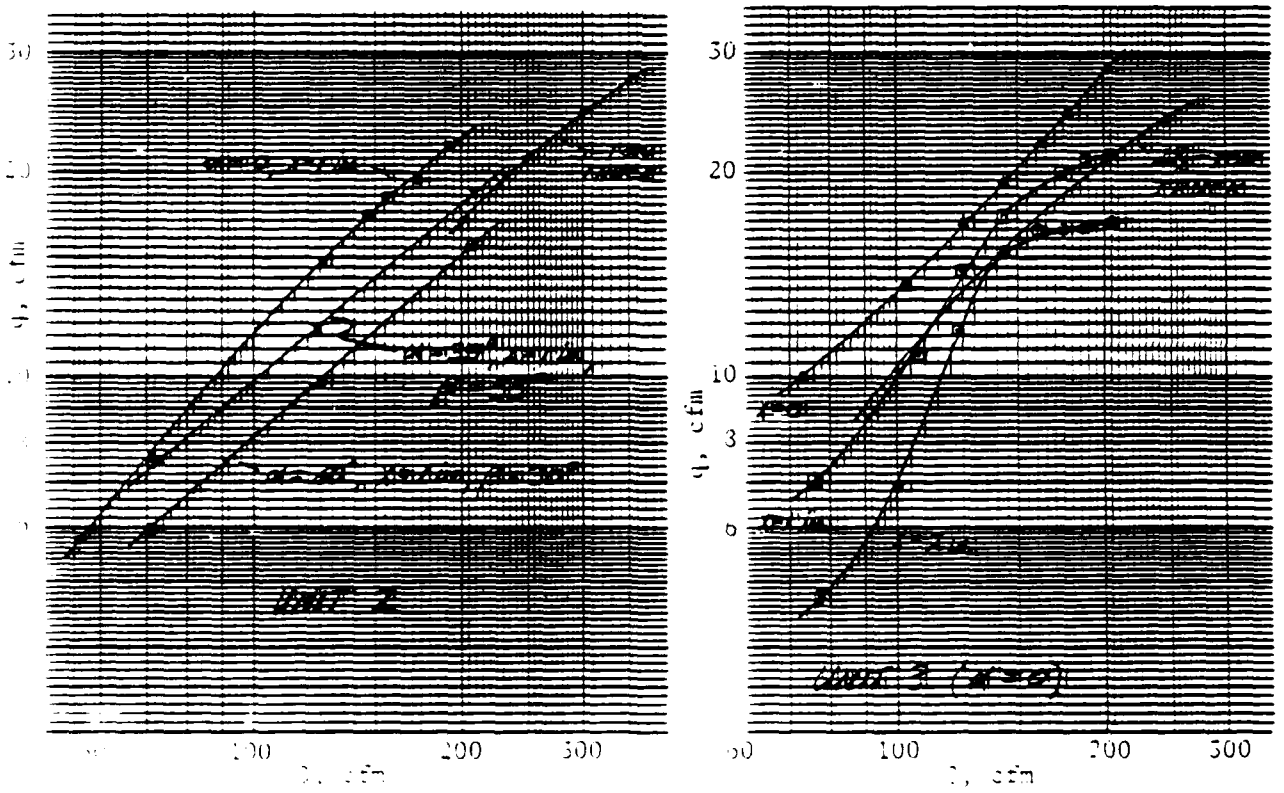

Figure 5-35. Comparison of On-Vehicle Flow Data with Selected Laboratory Data. On-Vehicle Measurements Made With Engine Compartment Open.

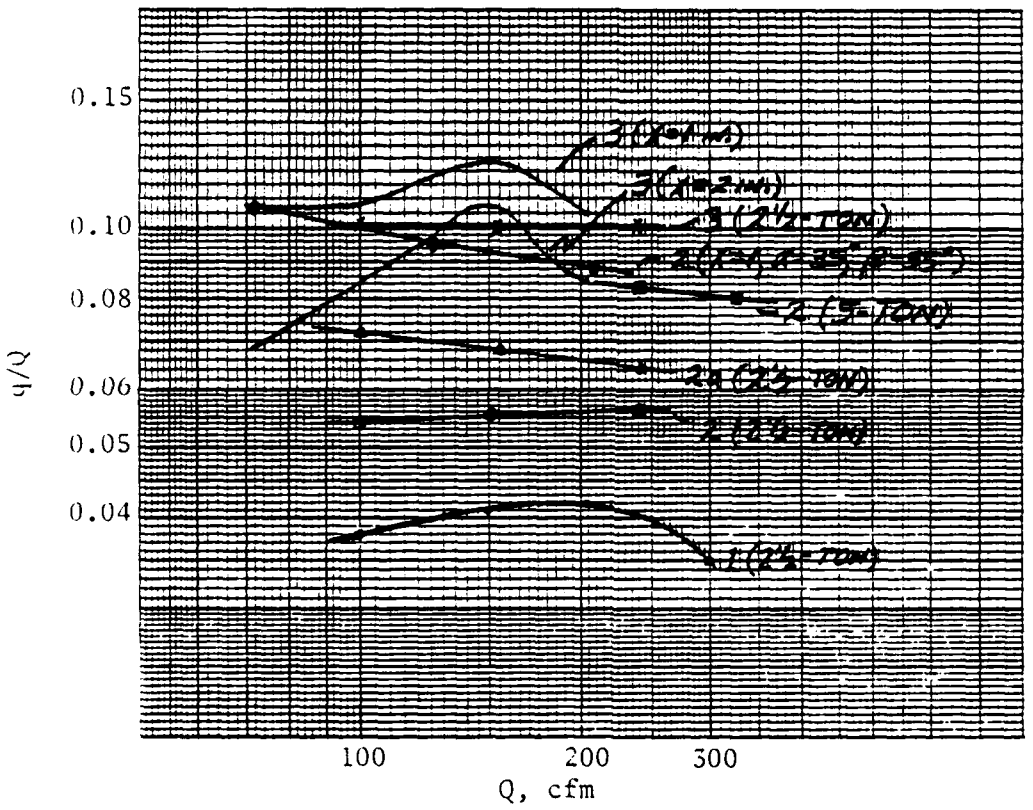

Figure 5-36. Ratio q/Q for On-Vehicle Flow Data and Selected Laboratory Data. On-Vehicle Measurements Made With Engine Compartment Open.

that **q** may remain relatively level at about 12 cfm for Q > 100, and that **q** for the uncoupled case may approach this level for higher Q. This is not entirely inconsistent with the curves for units 2 and 3 shown in Figures 5-18 and 5-19, where the increase in secondary flow with Q is much smaller once a certain value of Q is exceeded. The critical value tends to decrease with increasing separation.

In considering the previous results, it is important to remember that the fan-airpumps used in this program were off-the-shelf units that were not designed nor optimized for the applications or vehicles investigated. By using these units, however, and by being able to develop a reasonable correlation between the on-vehicle measurements and the laboratory data, it is possible to assess fan-airpump potential in terms of the air cleaner's flow requirements. In making this assessment, it is necessary to consider both the laboratory and on-vehicle data in terms of the secondary flows required by the air cleaner system. Traditionally, the secondary flow requirement is specified as 10 percent of the rated primary flow. In this case, if the air cleaners on the 2½- and 5-ton trucks were scavenged, the maximum secondary flow requirement would be 41 and 55 cfm respectively. As will be discussed later, the need for 10 percent scavenging may be questionable; laboratory tests having shown good results with scavenging as low as 5 percent.

The ratios of **q/Q** required of a fan-airpump to meet the 5-10 percent scavenging requirement for the 2½- and 5-ton truck are shown in Figure 5-37. These curves show that the requirements for both vehicles are similar, about 0.17 at 10 percent and 0.085 at 5 percent. **q/Q** for unit 3 was ~0.10 for the 2½-ton truck, while **q/Q** for unit 2 on the 5-ton truck was 0.08. Unit 3 was not tested on the 5-ton truck, but probably would have shown better results than unit 2. Based on these data, it is likely that a properly designed and interfaced fan-airpump could meet the scavenging requirements for the 2½-and 5-ton trucks, provided ducting losses remain small. It should be remembered, however, that the laboratory and on-vehicle data represent secondary flow development at locations where primary flow velocities were maximized. As it turns out, these locations are fortuitous in that they are accessible and relatively close to the air cleaner. This will minimize the impact of duct configuration on secondary flow development, as examined in the next section.

It should also be noted that secondary flow development, in terms of **q/Q,** can be improved by changing the inlet design and by the method of interfacing with the fan shroud; ratios on the order of 0.15 were obtained with units 2 and 3, when directly coupled. The use of two fan-airpumps per vehicle also represents a reasonable method for increasing secondary flow, if necessary.

5.2.5. **The Impact of Duct Configuration on Secondary Flow.** A series of tests was conducted to determine the impact of duct configuration on secondary airflow development. These tests were run on unit 4 (Table 5-1), arranged as shown in Figure 5-38. During testing, 11 configurations were evaluated in addition to the baseline case. Experimental results are shown in Figures 5-39 and 5-40. Figure 5-39 shows scavenging vacuum in the secondary flow line as a function of the primary dynamic pressure. In this case, curve 1 represents the baseline configuration. Each configuration tested is defined in Table 5-3. Larger

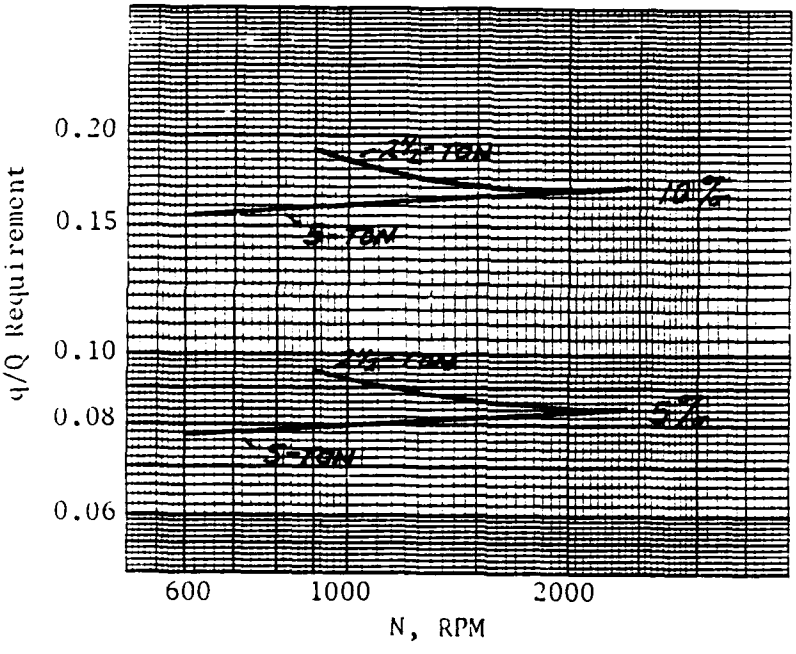

Figure 5-37. q/Q Requirement for 5- and 10-Percent Scavenge as a Function of Engine Speed on 2-1/2- and 5-ton Truck.

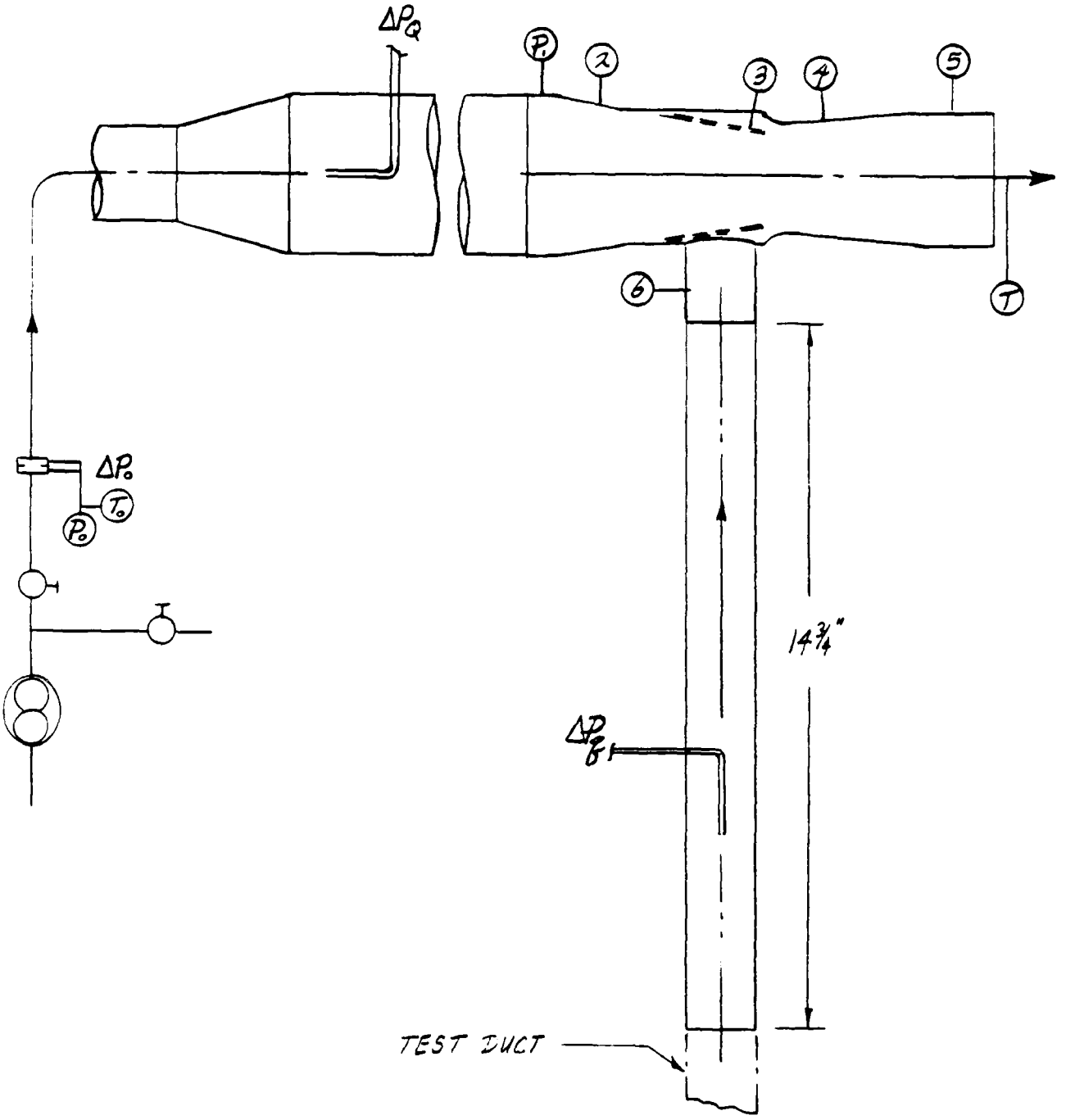

Figure 5-38. Test Arrangement for Studying the Impact of Duct Configuration on Secondary Flow Development (Unit 4).

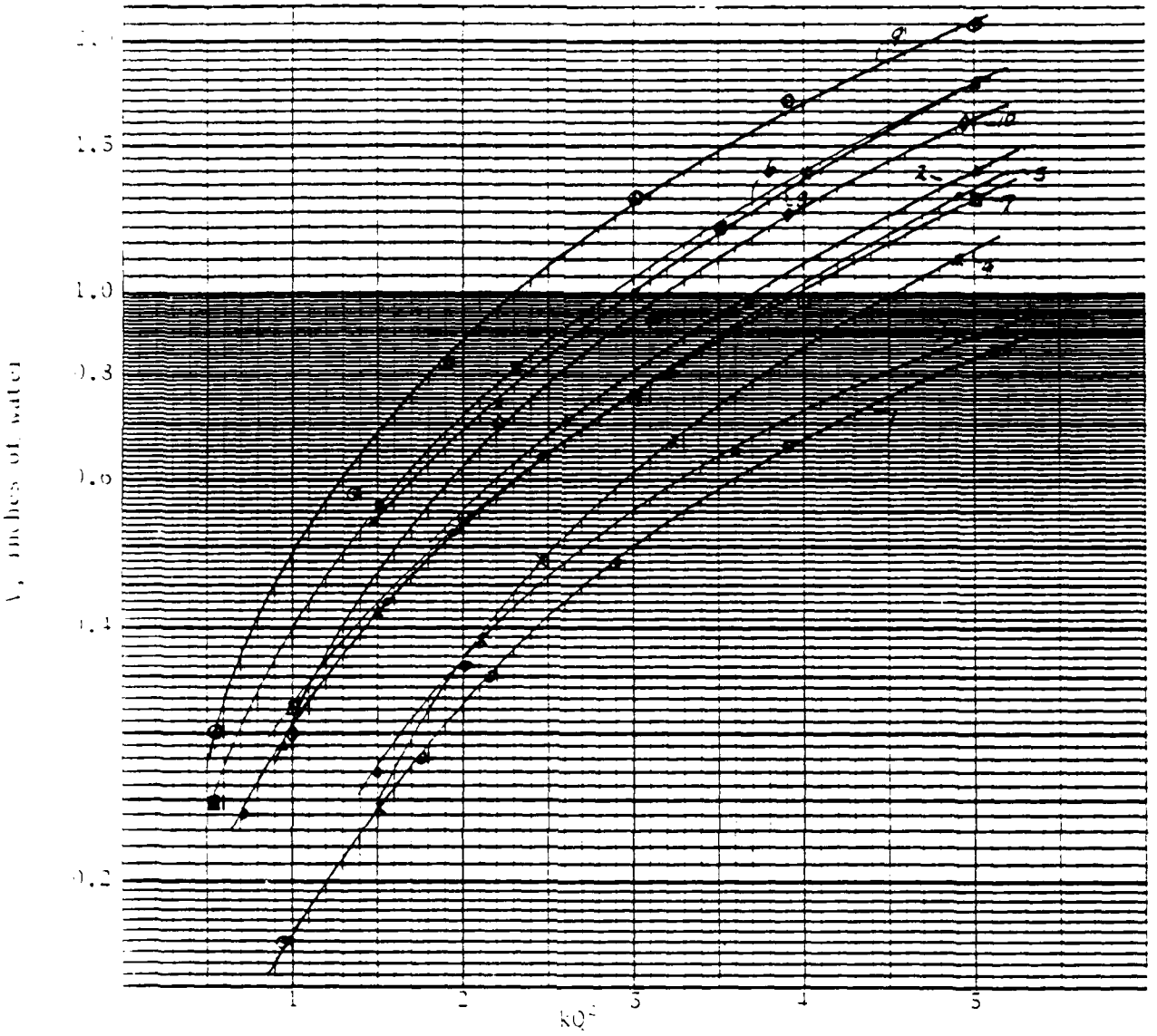

Figure 5-39. Scavenging Vacuum V as a Function of Inlet Dynamic Pressure and Duct Configuration (Unit 4).

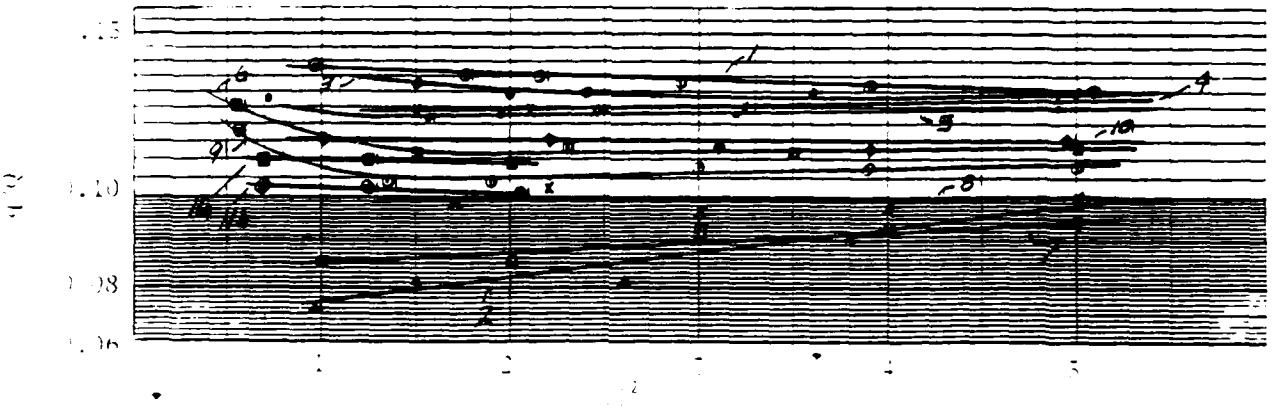

Figure 5-40. a/Q as a Function of Inlet Dynamic Pressure and Duct Configuration (Unit 4).

Table 5-3. Secondary Duct Configurations for Airflow Study (Unit 4)

Configuration	Description
1	Baseline (reference Figure 5-38)
2	90° copper elbow at entrance, 2½-inch radius at centerline
3	35-inch smooth rubber hose
4	71-inch smooth rubber hose
5	107-inch smooth rubber hose
6	70-inch smooth rubber hose + 90° copper elbow + 35-inch smooth rubber tube
7	Sharp 90° elbow at entrance
8	120-inch EPDM* Elastomer wire-reinforced hose in large sweep elbow 
9	35-inch smooth rubber tube + 90° copper elbow + 35-inch smooth hose + 90° copper elbow + 35-inch smooth hose
10	35-inch smooth rubber tube + 90° copper elbow + 35-inch smooth rubber tube
11	55-inch EPDM* Elastomer hose Type 494
a.	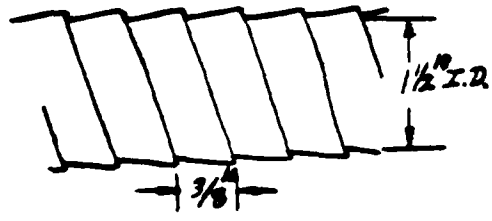
b.	direction of q reversed

NOTE: All configurations added to baseline are as shown in Figure 5-38. The first item interfaced to baseline.

*Ethylene Propylene Diene Monomer, manufactured by the Ohio Rubber Company.

negative scavenge pressures for a given dynamic pressure correspond to decreasing levels of secondary flow. Figure 5-40 shows the ratio q/Q as a function of primary dynamic pressure, kQ^2. These data correlate well with the data in Figure 5-39 and show that q/Q is relatively constant for a given duct geometry.

Another way to examine the effect of duct geometry on secondary airflow is to look at the apparent friction factor for a given duct geometry compared to the friction factor for the baseline case. The concept of friction drag and the relationship between duct pressure loss and friction drag is based on equations that define the shear stress acting on the internal surface of a duct when a known velocity exists at the duct wall. Downstream of the entrance region, the velocity gradient is independent of duct length. Here the shear stress causes a force along the wall that is proportional to the area in contact with the fluid. This force is usually referred to as drag, or friction.

In classical aerodynamic theory, the drag force acting on surface A is expressed as:

$$F_D = C_D P_D A \tag{10}$$

where: C_D = drag coefficient
P_D = dynamic pressure, $\frac{1}{2}\rho V^2$
A = surface area

For a round duct, $A = \pi d\ell$, where ℓ is duct length, hence:

$$F_D = C_D P_D d\pi\ell \tag{11}$$

In order to develop and maintain flow, this drag or friction must be overcome by a pressure force corresponding to the duct pressure drop. As such,

$$C_D P_D d\pi\ell = A\Delta P_t \left(\frac{\pi d^2}{4}\right) \tag{12}$$

where ΔP_t is the total pressure loss in the duct. Solving for ΔP_t gives:

$$\Delta P_t = C_D P_D \left(\frac{4\ell}{d}\right) \tag{13}$$

In duct flow, C_D is replaced by the symbol f, the Darcy friction factor. Since the shear stress at the wall reaches a constant value for pipe flow in equilibrium, the friction factor is also constant once equilibrium is reached. Also, since the shearing stress caused by a gas, at normal temperature and pressure, is proportional to the velocity gradient that exists normal to the direction of flow, it follows that any change in the velocity profile will cause a loss of energy and result in a corresponding pressure loss in the pipe. A change in pipe roughness, for instance, changes the velocity profile at the wall. This, in turn, changes the shear stress and the friction factor. Since the same is true for changes in direction, cross-sectional area, or shape, it is clear that duct configuration could have a significant impact on secondary flow development and overall fan-airpump performance.

Rearranging equation 13, the friction factor becomes:

$$f = \frac{1}{4}\left(\frac{\Delta P_T}{P_D}\right)\frac{d}{\ell} \tag{14}$$

For established flow, the change in total pressure along the pipe is equal to the change in static pressure measured at the wall. Since the dynamic pressure P_D is equal to $\frac{1}{2}\rho V_2$, where V is the average velocity in the duct, P_D must be corrected with respect to the velocity profile and the point of measurement. Since P_D was measured at the centerline, the correction factor over our range of interest (NR_E 20,000 - 50,000) is derived from the expression $V/V_{max} = 0.8$. The Darcy friction factor as a function of the experimental data then becomes:

$$f_D = \frac{1}{4}\,\frac{d}{\ell}\left(\frac{1}{.8}\right)^2 \frac{\Delta P_1}{\Delta P_2} \tag{15a}$$

which gives:

$$f'_D = 0.035\ \Delta P_1/\Delta P_2 \tag{15b}$$

where: ΔP_1 = pressure drop in the tube; in water
ΔP_2 = dynamic pressure in the tube; in water

when normalized to the baseline case. Although f'_D is not a true friction factor, it is convenient for comparing the effects of duct configuration on secondary flow based on the experimental data.

The Reynolds number within the duct can also be expressed in terms of the dynamic pressure:

$$NR_E = \rho\frac{dv}{\mu} = 1097.76\ \frac{d}{\mu}\sqrt{\rho\Delta P_2}\,(.8) \tag{16}$$

where: ρ = air density, lb_m/ft^3
d = tube diameter, inches
μ = air viscosity, poise
ΔP_2 = pitot tube pressure, inches water
0.8 = correction factor for V/V_{max}

For the experimental data at hand, the Reynolds number becomes:

$$NR_E = 2.705 \times 10^4\ d\sqrt{\Delta P_2} \tag{17}$$

The turbulent flow friction factor for a straight pipe can be approximated from the modified Colebrook equation,

$$f_{D_1} = \frac{1}{4}\log^{-2}\left[\frac{\varepsilon/D}{3.7} + \frac{13}{NR_E}\right] \tag{18}$$

where ε/D is the relative roughness factor and NR_E is the local Reynolds number. The Darcy friction factor, f'_D, is four times the Fanning friction factor, which is also widely used. The factor ε/D accounts for pipe roughness. This equation has a maximum error of 0.75 percent with respect to the implicit Colebrook equation for $NR_E \sim 30{,}000$ or greater and $\varepsilon/D > 0.004$.

For smooth pipes, for NRE = 10,000 to 200,000, the Darcy friction factor can also be approximated as:

$$f_{D_1} = \frac{4(0.046)}{NR_E^{0.2}} \tag{19}$$

In order to know whether the boundary layer flow is likely to be laminar or turbulent, the Reynolds number for the flow in the pipe must be considered. Flow conditions in a smooth closed channel will usually be laminar if the Reynolds number (based on hydraulic diameter) is less than 2,000 and turbulent if above 4,000. For values between 2,000 and 4,000 the flow is considered transitional. It has already been noted that our area of interest is in the turbulent range, with Reynolds numbers likely to be on the order of 15,000 - 30,000.

Values of f_{D_1} and f_{D_2} are shown in Figure 5-41 for Reynolds numbers up to about 60,000. Standard curves based on data from a number of investigators are included for comparison. An examination of these curves shows the simpler expression f_{D_1} is sufficiently accurate when smooth tubing is used, while the more complex equation f_{D_2} is better suited for ducts with rougher surfaces.

By using equation 19, Darcy friction factors can be calculated directly from the experimental data.

$$f'_{D_1} = \frac{0.024}{\sqrt[5]{d^{10}\sqrt{\Delta P_2}}} \tag{20}$$

$$f'_{D_2} = \frac{1}{4}\log^{-2}\left[\frac{\varepsilon/D}{3.7} + \frac{4.806 \times 10^{-4}}{d\sqrt{\Delta P_2}}\right] \tag{21}$$

The data can then be plotted as a function of main flow dynamic pressure kQ^2 to show the apparent friction factor in the secondary duct as a function of primary flow. Since these values assume a straight duct without entrance and exit losses, the curves represent the friction factor that would occur for flow in an equivalent straight tube at dynamic pressure ΔP_2. Comparison of these values with the ideal case will indicate to what extent the effective friction factor is increased to account for specific duct geometries.

Values for f'_D and f'_{D_1} calculated from equations 15b and 20 are given in Figure 5-42 as a function of kQ^2. These data clearly show the impact of duct configuration on secondary flow development. For all values of kQ^2, it is clear that the 90° bends dominate the secondary flow and that bends located near the entrance are more severe than midstream bends. Tube roughness also turned out to be an important parameter.

5.2.6. **Summary of Findings for Secondary Flow Development.** From a practical point of view, the results are encouraging. First, examination of the fan-airpump's design indicates that its configurations can be optimized to improve secondary flow response. Second, on-vehicle airflow measurements for the 2½- and 5-ton trucks indicate that air with sufficient volume and dynamic pressure is available for satisfactory fan-airpump operation. Finally, the proximity of proposed fan-airpump locations with respect to the air cleaner assemblies on both vehicles indicates that only minor duct losses will be experienced in connecting the secondary port to the air cleaner.

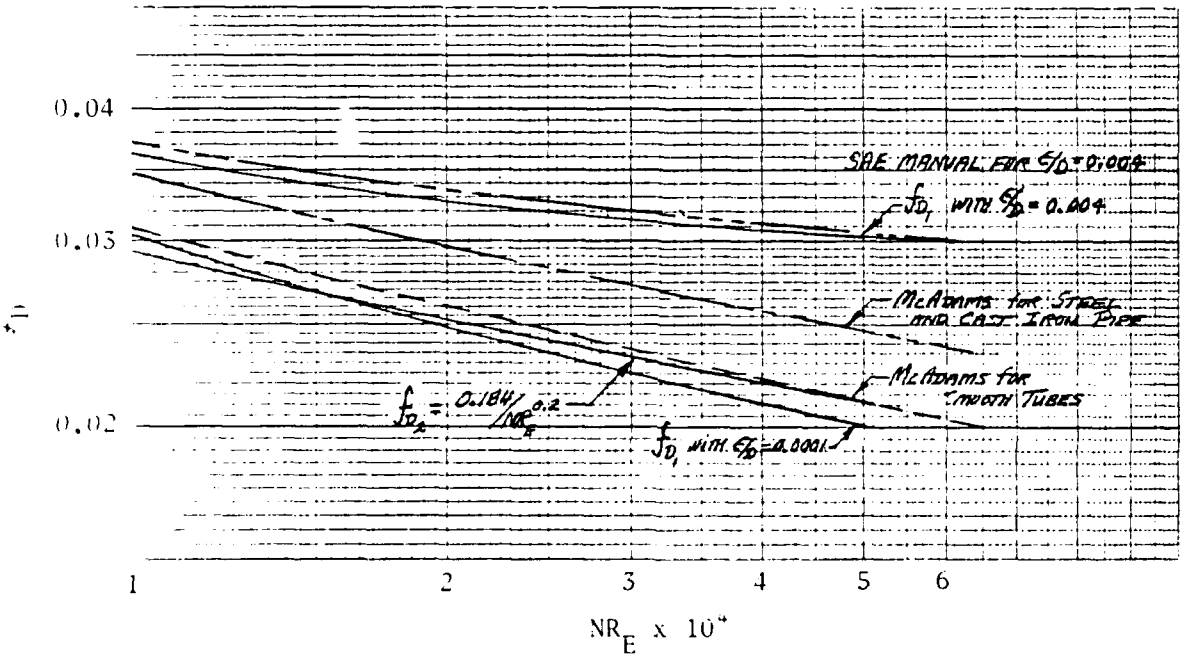

Figure 5-41. f_{D_1} and f_{D_2} as a Function of Reynolds Number NR_E

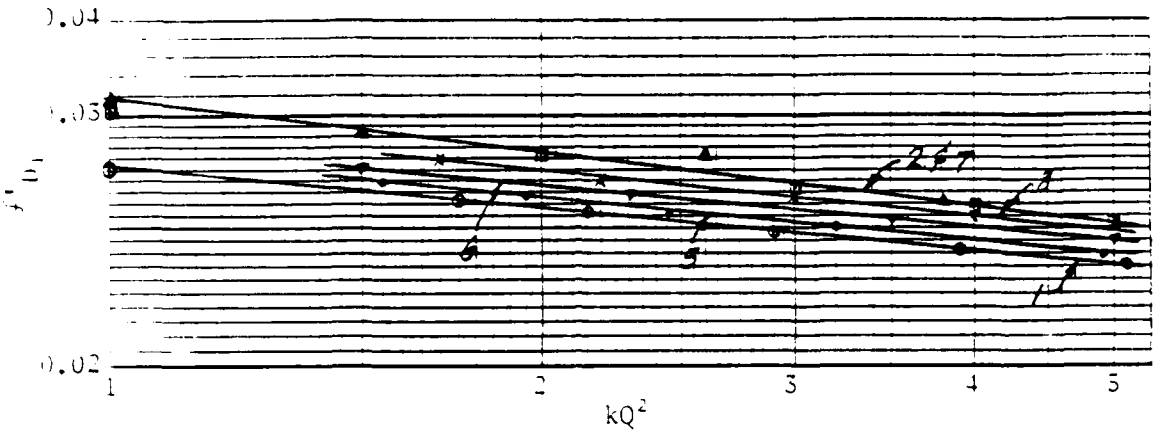

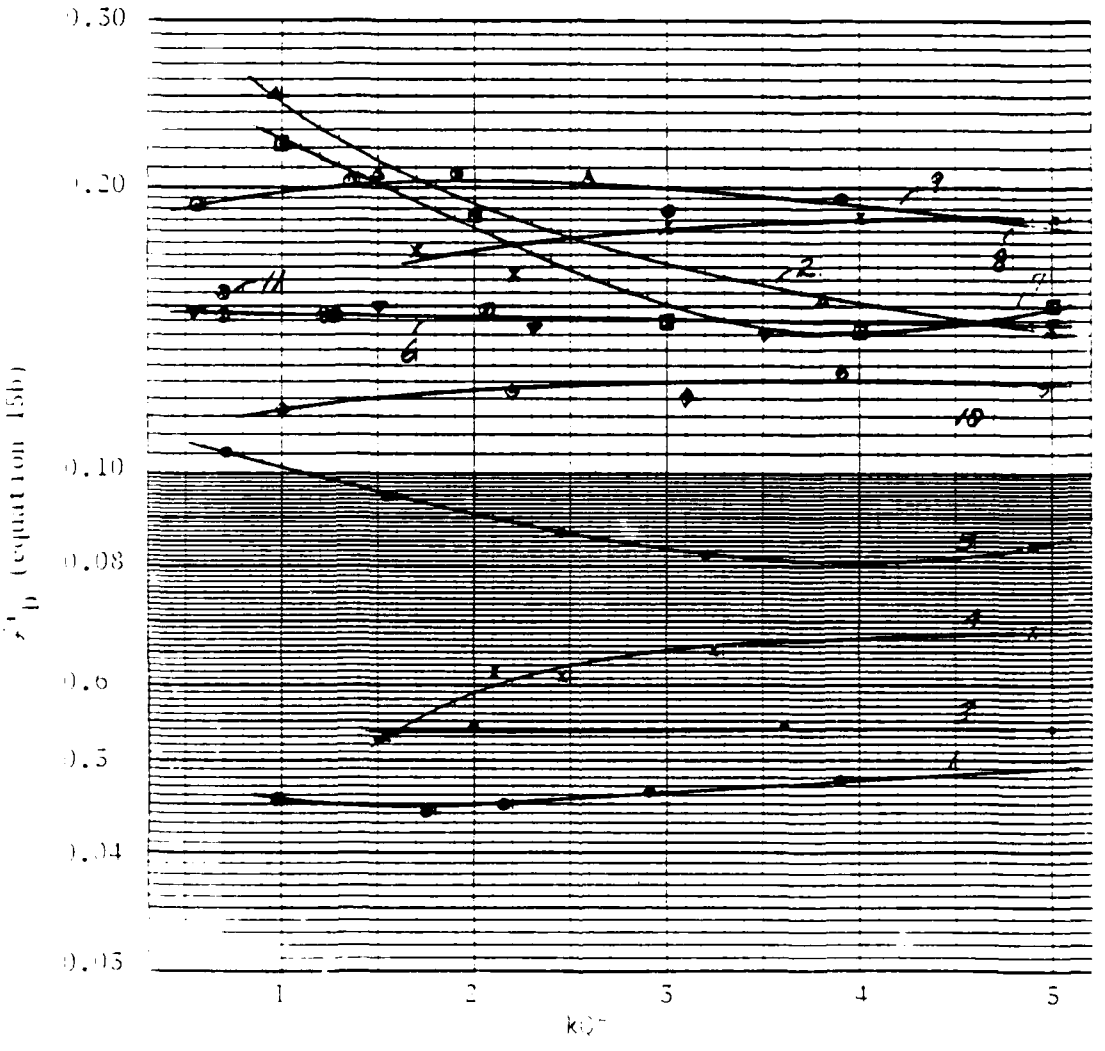

Figure 5-42. f'_D and f'_{D_1} as a Function of Inlet Dynamic Pressure and Duct Configuration (Unit 4).

5.3. Laboratory Testing with 2½- and 5-Ton Truck Air Cleaner Systems

Laboratory tests were conducted using the fan-airpump in conjunction with the air cleaners used on the 2½- and 5-ton trucks. Since the 2½-ton truck system is a single-stage filter element, various precleaners were added during testing. A typical test arrangement is shown in Figure 5-43. Fan air for the fan-airpump was produced with a blower, which was adjusted to simulate different operating conditions. Baseline data were obtained for the single-stage system and for the system with the precleaner operating with a scavenge blower, which is typical of many installations.

Results are shown in Tables 5-4 and 5-5. The primary flow rate for the tests covered by Table 5-4 was 480 cfm. This compares with a rated flow of 410 cfm, which was used for the tests shown in Table 5-5. For this reason, the results in Table 5-4 can only be used to show relative performance. These results are discussed first, independently of those given in Figure 5-5.

In general, the precleaner configured system provided increased service life, although to a lesser degree than expected because of the large initial ΔP at 480 cfm. Dust capacity with the military precleaner averaged about 730 grams on Coarse dust. For the 2070 precleaner, using a scavenge blower, capacity was 940 grams. For the 2070 p/c with fan-airpump No. 2, dust capacity averaged about 750 grams. These values compare with a baseline average of 590 grams (1.6 hours).

All testing with the fan-airpump (w/2070 p/c) except 8C, and with the blower on tests 6C and 7C (w/2070 and military p/c), was conducted with the scavenge flow set to approximately 40 percent of the rated scavenge flow, based on the primary flow rate (i.e., 6C: $q/Q = {}^{20.5}/_{480} = .43 = .43({}^{48}/_{480})$, where the rated scavenge flow equals 10 percent of the rated primary flow). For tests 1C - 5C, the scavenge flow was set to approximately 85 percent of the rated scavenge flow. From these results and from the theoretical model that was developed to investigate service life (see 5.4), it can be concluded that:

- service life can be extended by adding a precleaner to the 2½-ton truck system,
- precleaner design and optimization with respect to the air cleaner system is important to maximize service life,
- scavenge airflows that are less than the usual 10 percent of rated primary flow appear to be satisfactory, although the range was not defined, and
- a significant increase in overall initial restriction without a corresponding increase in precleaner efficiency is detrimental to service life.

The results shown in Table 5-5 for the 2½-ton truck support these conclusions.

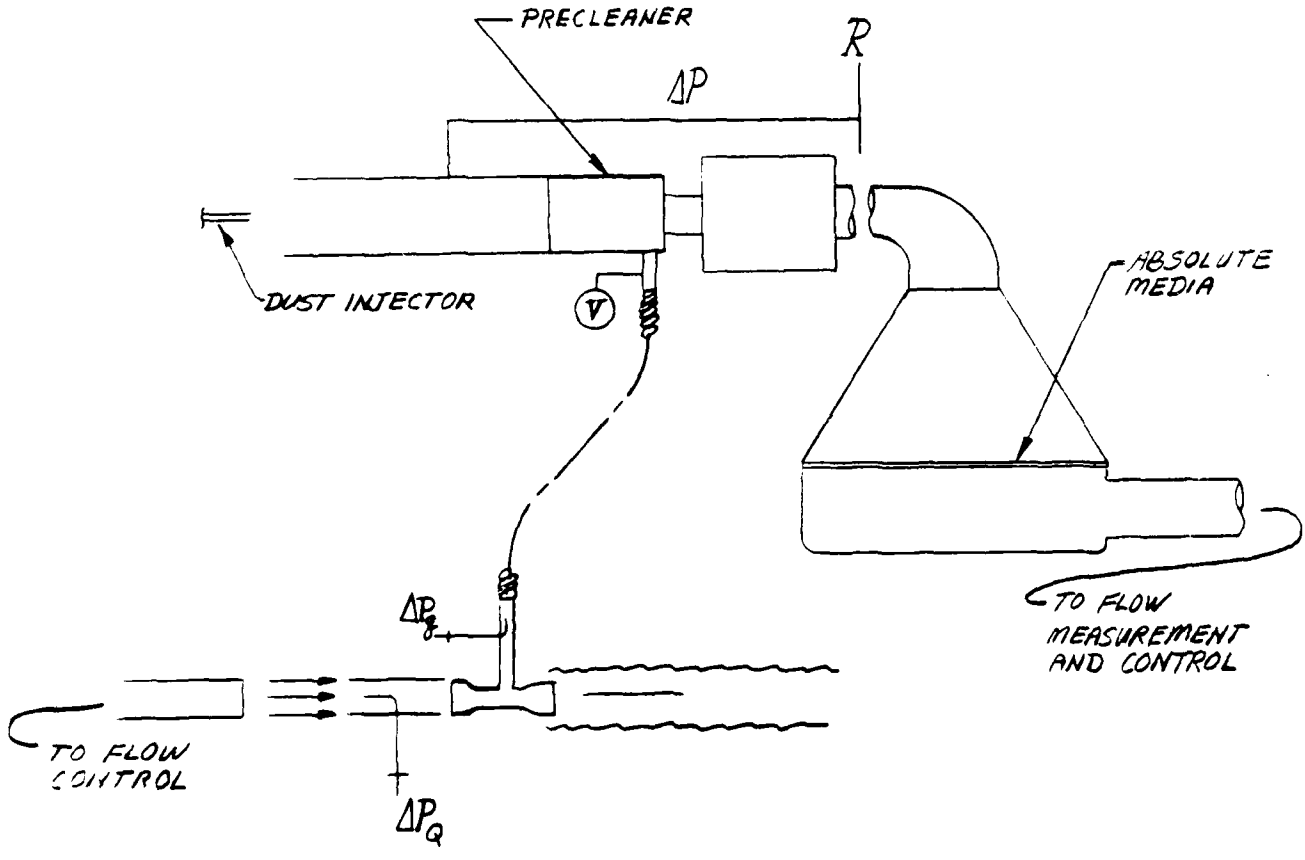

Figure 5-43. Test Arrangement for Measuring Air Cleaner Performance With Fan-Airpump Scavenge

Table 5-4. Relative Performance of 2½-Ton Truck Air Cleaner System with Precleaner and Fan-Airpump

(Main Airflow Rate: 480 CFM)

Test No.	Precleaner	Scavenge Source	Scavenge Flow-cfm	Initial P, "WG	Dust[1] Capacity, g	Capture[6] Efficiency of F/A, %	Overall[7] Efficiency %	Filter[8] Efficiency %
1C	Military[3]	Blower	41.0 (35)[5]	13.6	315[4]		---	---
2C	Military	Blower	41.0	14.0	710		99.64	96.31
3C	Military	Blower	41.0	13.8	740		99.61	96.00
4C	2060PC	Blower	41.0	17.5	270		99.27	93.81
5C	2070PC	Blower	41.0	12.5	845[4]		99.70	97.89
6C	2070PC	Blower	20.5 (43)	13.0	940		99.86	99.12
7C	Military	Blower	20.5 (43)	15.3	734		99.83	98.48
8C	2070PC	F/A #2	NIL	12.8	545		99.46	98.80
9C	2070PC	F/A #2	18.2 (38)	12.4	820	71 @ 1"	---	---
10C	2070PC	F/A #2	20.1 (42)	13.0	672	77 @ 1"	---	---
11A	None	N/A	N/A	7.2	730		99.86	99.86
22A	None	N/A	N/A	7.0	370[4]		98.78	98.75
23A	None	N/A	N/A	7.0	380[4]		98.41	98.40
24A	None	N/A	N/A	7.0	380[4]		99.24	99.24
25A	None	N/A	N/A	6.8	370[4]		99.36	99.35
30A	None	N/A	N/A	7.0	573		99.50	99.49
31A	None	N/A	N/A	7.2	605[2]		99.28	99.26
31AA	None	N/A	N/A	7.3	590[2]		99.59	99.58
32A	None	N/A	N/A	7.0	595[2]		98.62	98.52

(1) AC Coarse Dust @ 369 g/hr
- SAEJ726C cycle w/5-min steps; (2) w/10 min steps
- SAE Dust Nozzle
- SwRI Tray Dust Feeder
- Constant scavenge flow rate
- Dust capacity @ 20" H_2O ΔP

(3) GFE

(4) AC Fine Dust
Fan Airpump 5-1/4 feet from precleaner with two 90° bends (1-~10" rad.; 1~4" rad.), 1½-inch hose

(5) Percent of rated scavenge flow for given main flow

(6) Percent of blower output flow captured by fan-airpump inlet

(7) $\left(1 - \frac{\text{penetration}}{\text{dust feed}}\right) \times 100$

(8) $\left(1 - \frac{\text{penetration}}{\text{wt. gain + penetration}}\right) \times 100 = \left(\frac{\text{wt. gain}}{\text{wt. gain + penetration}}\right) \times 100$

Table 5-5. Relative Performance of 2½- and 5-Ton Truck Air Cleaner Systems with Fan-Airpump

(Main Airflow Rate: 410 cfm)

Test No.	Vehicle Type	Precleaner	Scavenge Source	Initial ΔP, "WG	Efficiency	Dust[1] Capacity, g	Cycle [2]
53A	2½-ton	---	---	5.5	99.93%	875	5-min variable[4]
54A	2½	---	---	6.0	98.81*/98.98	820	30-min Fine dust*; then 5-min variable
55A	2½	Military[3]	Blower	10.8	99.91	1820	5-min variable
56A	2½	Military[3]	Blower	10.8	99.92	1990	10-min variable
57A	2½	2070	Blower	10.3	---	1890	10-min variable
11C	2½	2070	#2A+#3	10.4	99.48	1590[7]	10-min variable
14C	2½	2070	#2A+#3	9.5	99.93	2100[11]	10-min variable
15C	2½	2070	#2A+#3	9.8	99.91	1495	10-min variable
16C	2½	2070	#2A+#3	10.3	99.90	1220	10-min variable
17C	2½	2070	#3+#4	10.7	99.96	1365	10-min variable
18C	2½	2070	#4	10.3	99.92	1475	10-min variable
8b	5-ton	2070[5]	Blower	6.1	99.95	12,730	5-min varaible[9]
9b	5	2070	#2A+#3	5.1	99.99	10,230[6]	5-min variable
10b	5	2070	#2A+#3	5.0	99.99	10,550	5-min variable
12c	5	(8)	#2A+#3	3.4	99.96	8,070[7]	10-min variable
13c	5	(8)	#2A+#3	3.4	---	10,535	10-min variable
13b	5	(10)	---	3.7	99.99	10,770	10-min variable
12b	5	(10)	---	3.7	99.99	11,490[11]	10-min variable
14b	5	(10)	---	3.7	99.99	12,260[11]	10-min variable

(1) AC Coarse dust unless otherwise noted
(2) SAE type cycle
(3) GFE
(4) 369 g/hr
(5) Element in housing, without internal precleaner
(6) #3 fan-airpump became disengaged during test
(7) Fan-airpump outlets restricted slightly
(8) Modified 5-ton housing with scavenge ports added
(9) 495 g/hr
(10) Std. 5-ton housing with internal precleaner
(11) Powder Technology Incorporated SAE coarse dust

Results for the 5-ton truck are less definitive. No clear advantage was gained by scavenging the present housing or by adding a precleaner to a system where the 5-ton element was placed in a housing without an internal precleaner. However, scavenging did offer the advantage of keeping the house clean. Furthermore, it is likely that service life can be improved by redesigning the internal precleaner to take advantage of the secondary airflow or by properly matching an external precleaner to the 5-ton element.

5.4. Design Component and Component Integration Study

As discussed earlier, airflow measurements were made in the engine compartments on 2½- and 5-ton series trucks to determine if sufficient flow and pressure existed to permit satisfactory fan-airpump operation. Results showed that fan-airpumps could readily be applied to both vehicles, as far as the vehicle/fan-airpump interface characteristics were concerned. Another parameter that must be considered, however, is the overall effect on air cleaner performance, especially service life. In fact, it is this parameter that has led to the use of precleaners and consideration of the fan-airpump as a primary precleaner component.

The major reason for adding or incorporating a precleaner into an air cleaner system is to increase service life. This is done because the precleaner removes a large amount of dust that would otherwise have to be handled by the final filter. Since the pressure loss across the precleaner does not increase with time, the overall affect is to slow the pressure drop increase across the filter by lessening its dust burden over time. The improvement in service life, however, is not directly proportional to the performance of the precleaner. In fact, there are cases where service life is barely increased, even though precleaner efficiency is high. The reasons for this are associated with the increase in initial restriction caused by adding the precleaner and the relationship between the new initial restriction, the dust loading rate, and the final allowable restriction. The interaction of these parameters can be studied by developing a model to predict service life as a function of the dust concentration reaching the final filter. Two systems can be used, one consisting of a filter, the other consisting of a filter preceded by a precleaner. Service life for these systems is inversely proportional to the dust concentration X_f reaching the filter, and in the second case, also to a factor ($^1/\beta$) related to the incremental change in initial restriction caused by adding the precleaner:

$$L_1 \alpha {}^1/X_{f_1} \tag{22a}$$

$$L_2 \alpha {}^1/X_{f_1}({}^1/\beta) \tag{22b}$$

In terms of the amount of dust being introduced to the system X_o, the dust reaching the filter equals:

$$X_{f_1} = X_o \tag{23}$$

$$X_{f_2} = X(1 - \eta) \tag{24}$$

where η is the efficiency of the precleaner. The relative change in service life caused by adding the precleaner can then be written as:

$$\Delta L = \frac{L_2 - L_1}{L_1} = \frac{1 + \eta\beta - \beta}{(1 - \eta)\beta} \tag{25}$$

so that L_2 becomes:

$$L_2 = \frac{L_1}{(1 - \eta)\beta} \tag{26}$$

The impact of β and η on service life is shown in Figures 5-44 and 5-45. As can be seen, in the typical range of interest, service life is very sensitive to changes in efficiency for a given value of β. Conversely, minor improvements in efficiency will have little, if any, effect on service life if β must be increased significantly to increase efficiency.

It has been noted that β is related to the increase in initial pressure drop caused by adding the precleaner to the system. This is because increasing ΔP_i decreases the allowable pressure drop remaining for dust loading, since:

$$\Delta P_\ell + \Delta P_i = \Delta P_f = \text{a constant} \tag{27}$$

where:
- ΔP = ΔP available for dust loading
- ΔP_f = maximum allowable ΔP
- ΔP_i = initial (clean) ΔP

Quantitatively, the relationship among these variables and service life is illustrated in Figure 5-46. As can be seen, if adding the precleaner does not change the slope of the loading curve, for instance, by significantly reducing the dust concentration to the filter, life will decrease (L'_2, L'_3) because loading starts at a higher ΔP_i. However, if the loading slope is sufficiently reduced, then service life is improved because the decrease in dust concentration over time more than compensates for the increase in initial restriction.

It is convenient to assume that for equal particle size distributions, the slope will be proportional to the amount of dust reaching the filter, and therefore inversely proportional to the efficiency of the precleaner. In practice, if a precleaner is added to the system, the particle size distribution of the dust reaching the filter and the concentration as a function of particle size will change. This will affect life in two ways. First, since less dust reaches the filter, life will tend to increase. Second, if the filter is not redesigned, it will (probably) clog faster than normal when exposed to the smaller particle size distribution. This would tend to reduce service life. The net result, in general terms, is that overall service life will be increased by adding the precleaner, but not to the extent possible if the filter were also redesigned to accommodate the smaller particle size distribution. The model developed here assumes no loss in life due to the shift in the particle size distribution. This is reasonable since a filter that is matched to the new distribution will restore the balance, as far as particle size is concerned. β then is related primarily to the change in initial pressure drop, and as a first approximation can be written as:

$$\frac{1}{\beta} = \frac{\Delta P_f - \Delta P_x}{\Delta P_f - \Delta P_i} \tag{28}$$

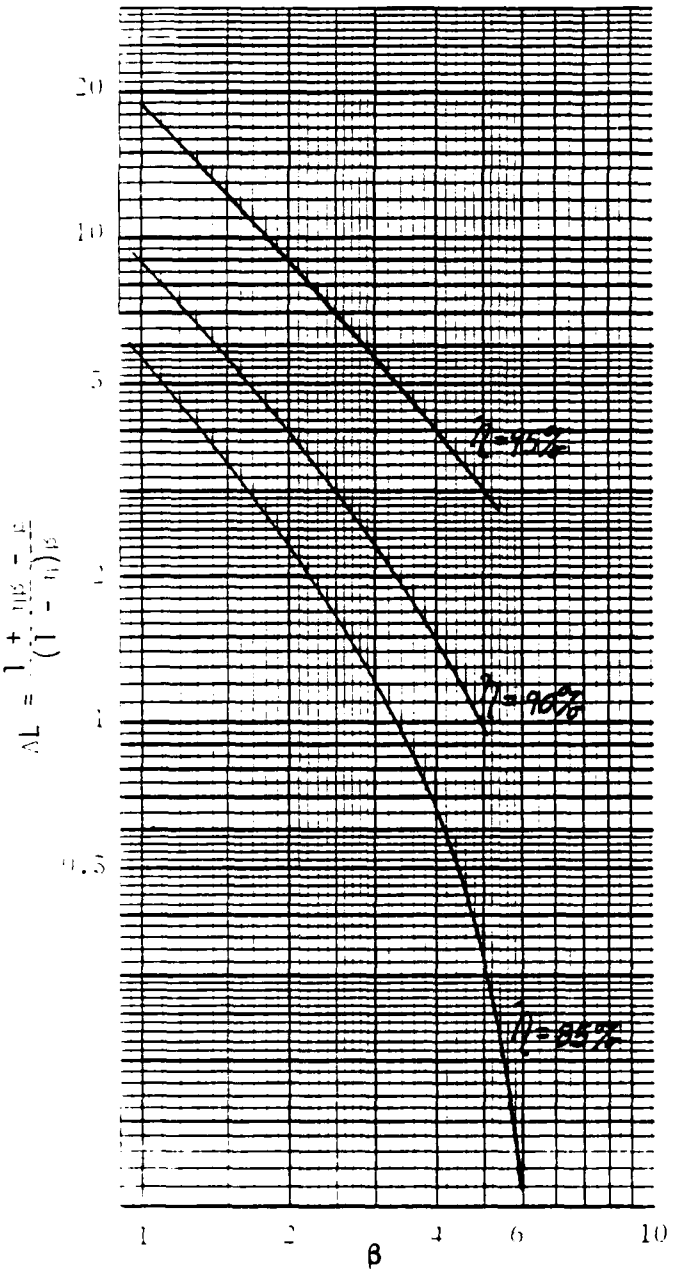

Figure 5-44. Relative Change in Service Life $(L_2 - L_1)/L_1$ as a Function of β and η

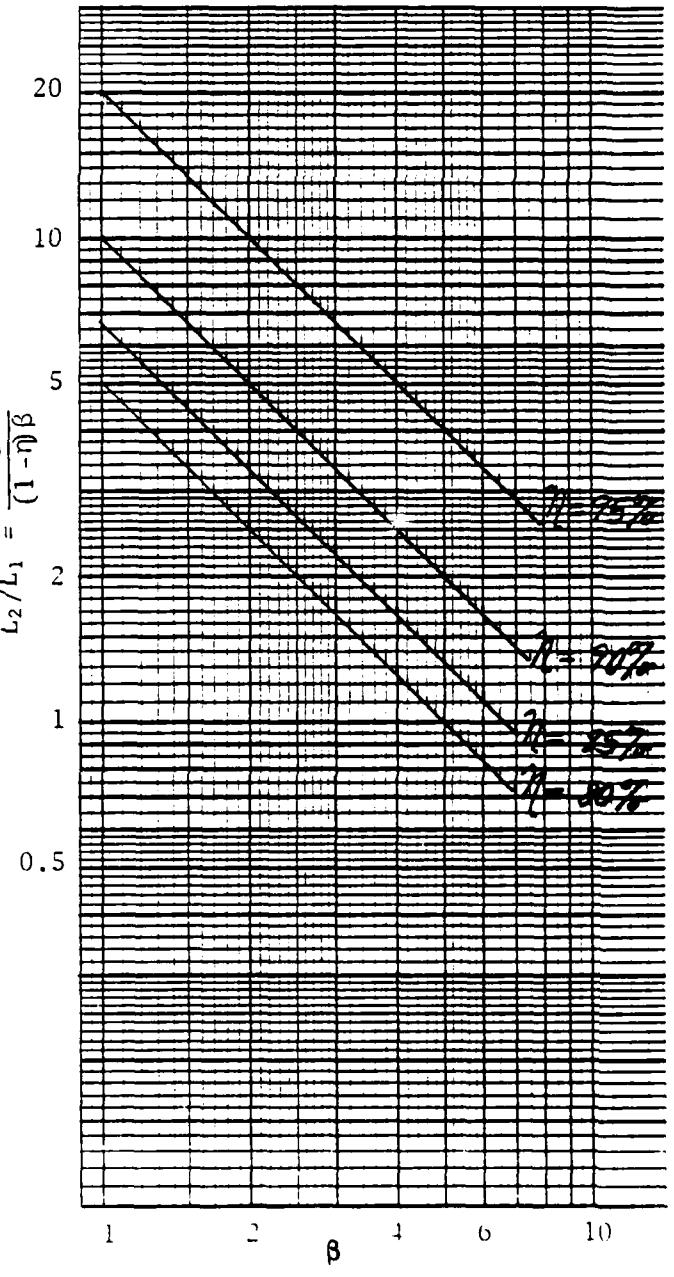

Figure 5-45. Ratio L_2/L_1 as a Function of β and η

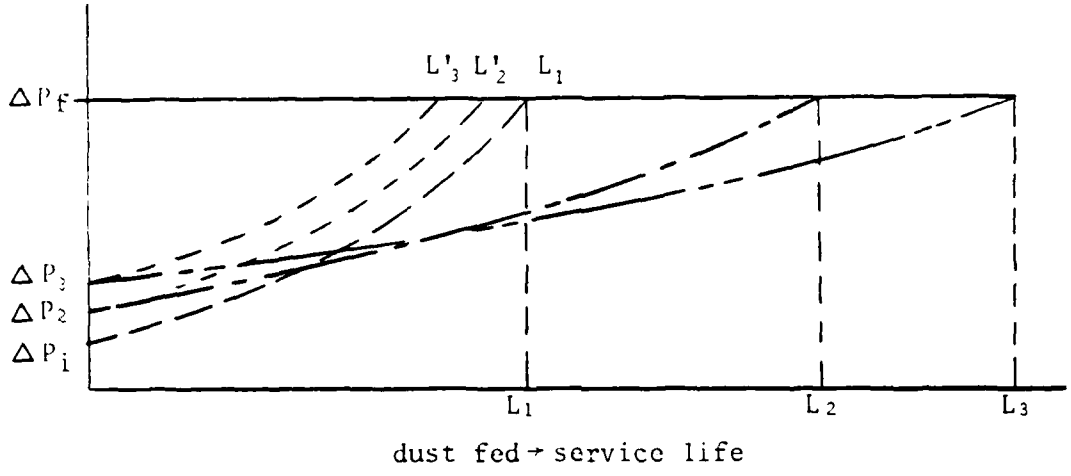

Figure 5-46. Relationship Between the Pressure Drop Variables and the Slope of the Dust Loading Curve and Service Life

where ΔP_x is the new initia' pressure drop caused by adding the precleaner, as shown in Figure 5-46. This shows that when:

$$\Delta P_x \rightarrow \Delta P_f \; ; \; \frac{1}{\beta} \rightarrow 0 \text{ and } L \rightarrow 0 \tag{29a}$$

$$\Delta P_x \rightarrow \Delta P_i \; ; \; \frac{1}{\beta} \rightarrow 1 \text{ and } L \rightarrow L_o \tag{29b}$$

For the case where adding the precleaner doubles the initial pressure drop, $\Delta P_x = 2\Delta P_i$. If $\Delta P_f = 4\Delta P_i$, which is quite reasonable, $1/\beta$ becomes 0.67, which means that service life would decrease 33 percent if there is no change in the loading slope. If loading is proportional to dust concentration, precleaner efficiency would have to exceed 33 percent to produce any gain in overall system life.

If precleaner efficiency is 85 percent, the dust reaching the filter is decreased by 85 percent, hence life should (intuitively) increase by a factor of 100/15 = 6.67, not taking into account the effect of initial pressure drop increase. When this factor is considered, it is found that life would only increase by a factor of 6.67 x .67 = 4.47. From equation 26, the new service life L_2 in this example becomes:

$$L_2 = \frac{L_1}{(1 - .85)} (.67) = 4.47 \, L_1 \tag{30}$$

If precleaner efficiency is increased from 85 to 95 percent, but at a cost of some increase in the initial pressure drop, the amount of dust reaching the filter is only 5 percent of the input dust, instead of 15 percent, hence:

$$L_3 \sim \frac{100}{5}\left(\frac{1}{\beta'}\right) L_1 \tag{31}$$

If $\Delta P'_x = 1.1 \, \Delta P_x$ (a 10 percent penalty in initial pressure drop in going from 85 to 95 percent efficiency), $1/\beta$ in the previous example becomes 0.6. This indicates that the life of the new system should be approximately 12 times the life before adding the precleaner, and about 2.7 times that when the 85 percent efficient precleaner was used. If $\Delta P'_x = 1.2 \, \Delta P_x$ (a 20 percent pressure drop penalty), these factors drop to 10.7 and 2.4 respectively. At $\Delta P'_x = 1.5\Delta P_x$, these factors are 6.7 and 1.5. Figure 5-47 shows L_2/L_1 and β as a function of $\Delta P_x/\Delta P_i$ for the hypothetical situation where $\Delta P_f = 4\Delta P_i$. For this case, $1/\beta$ equals:

$$\frac{1}{\beta} = \frac{4 - \Delta P_x/\Delta P_i}{3} \tag{32}$$

Again, these curves show that L_2 is very sensitive to efficiency η provided the pressure drop penalty is small. For example, for $\Delta P_x/\Delta P_i = 2$ and $\eta = 85$ percent, L_2/L_1 equals 4.4. If η can be increased to 90 percent while ΔP_x is only increased 10 percent from its current level, L_2/L_1 can be increased 35 percent to 6. Conversely, if a ΔP increase of 30 percent is required, then life remains constant even though efficiency was increased from 85 to 90 percent. However, if the 30 percent increase in ΔP were to produce a 95 percent efficiency, the theoretical L_2/L_1 factor would approach 9, twice the value at 85 percent efficiency. If β were not significant, one would expect L_2/L_1 with a 95 percent precleaner system to be three times that for a 85 percent precleaner system.

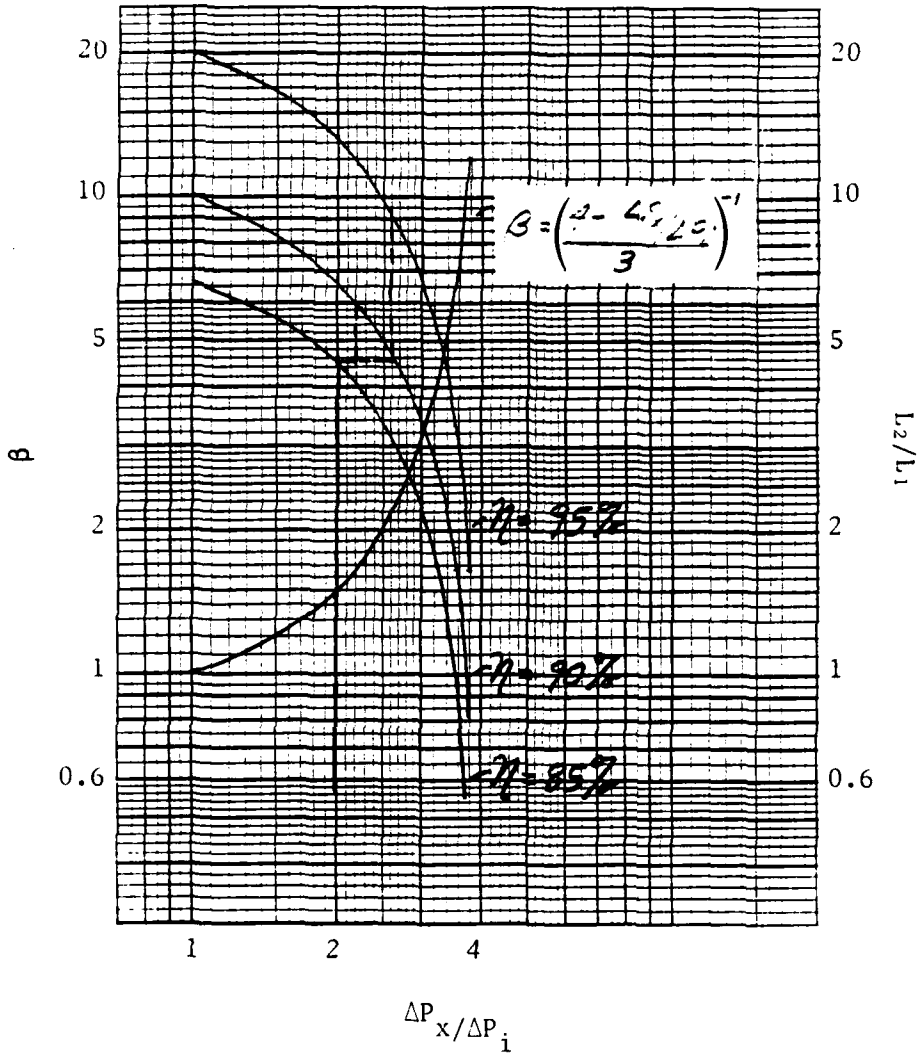

Figure 5-47. β and L_2/L_1 as a Function of $\Delta P_x/\Delta P_i$ and η

The theoretical model can be applied to the air cleaner system used on the 2½-ton truck. Currently, this system consists of as final filter for which $\Delta P_i \sim 5$ inches of water, while ΔP_f is 20 inches of water. For this system, $1/\beta$ becomes:

$$\frac{1}{\beta} = \frac{20 - \Delta P_x}{15} \tag{33}$$

which for $9 \leq P_x \leq 11$ gives $1.36 \leq \beta \leq 1.67$. L_2/L_1 over this range of β is given in Table 5-6 for η = 85, 90 and 95 percent.

Since ΔP_x increases as η increases, it may be reasonable to look along the diagonal to estimate the potential for improving service life. These data are shown in Figure 5-48. Values of L_2/L_1 achieved during laboratory testing, using two different precleaners operating at 10 percent scavenge flow, were on the order of 2 to 2½ with β on the order of 1.3 to 1.4. These values compare fairly well with the theoretical values in Figure 5-48 for these βs, suggesting precleaner operation in the lower efficiency range. It is important to note that the precleaner was not matched to the 2½-ton unit nor was the filter element adjusted for the change in particle size distribution. By optimizing design parameters, greater improvements in service life should be possible.

5.5. Cost Benefit Analysis and Economic Assessment

In 1983, a study was conducted to identify areas affecting the Operating Time to Failure (OTTF) for blower motor assemblies used with air cleaners on M48, M60, M109, M110, M551, M578, and M728 vehicles[1]. This study was initiated because blower motors on these vehicles were experiencing a much lower OTTF than specified, and as a result, more money and manpower was required to maintain air cleaner operability. Based on data which looked at blower motor incidents, vehicle mileage accumulation, and average vehicle speed, values for mean operating time to failure were found to range from 213 to 506 hours (Table 5-7), compared with a minimum specification requirement of 800 hours.

Main causes of failure were identified as worn brushes, worn bearings, internal shorts, and wire and connector problems. In most cases, failures were caused by vibration and contamination by moisture and dust, and in many cases, particularly where short circuits accounted for a large percentage of failures, the moisture was attributed to vehicle cleaning with steam or high pressure water hoses. Two blower motor assemblies are used per air cleaner, with one or two air cleaner units being used per vehicle.

A blower motor assembly is shown in Figure 5-49. Typical vehicle installations are shown in Figure 5-50 (M48, M60, M728), Figure 5-51 (M551), Figure 5-52 (M109), and Figure 5-53 (M110, M578).

The consequences of a blower motor failure on air cleaner performance are significant. Without proper scavenging, filter life is greatly reduced because the filter element is now exposed to a much heavier dust stream. With both blowers operating properly, approximately 95 percent of the ingested dust is removed in the precleaner. With only one blower motor operational, perhaps 90 percent of the dust can still be removed. With neither blower operational, however, less than

Table 5-6. Theoretical Values for L_2/L_1 as a Function of β and Precleaner Efficiency η for 2-1/2-ton Truck System

η \ β	1.25	1.50	1.88
85	4.9	4.4	4.0
90	7.4	6.7	6.0
95	14.7	13.3	12.0

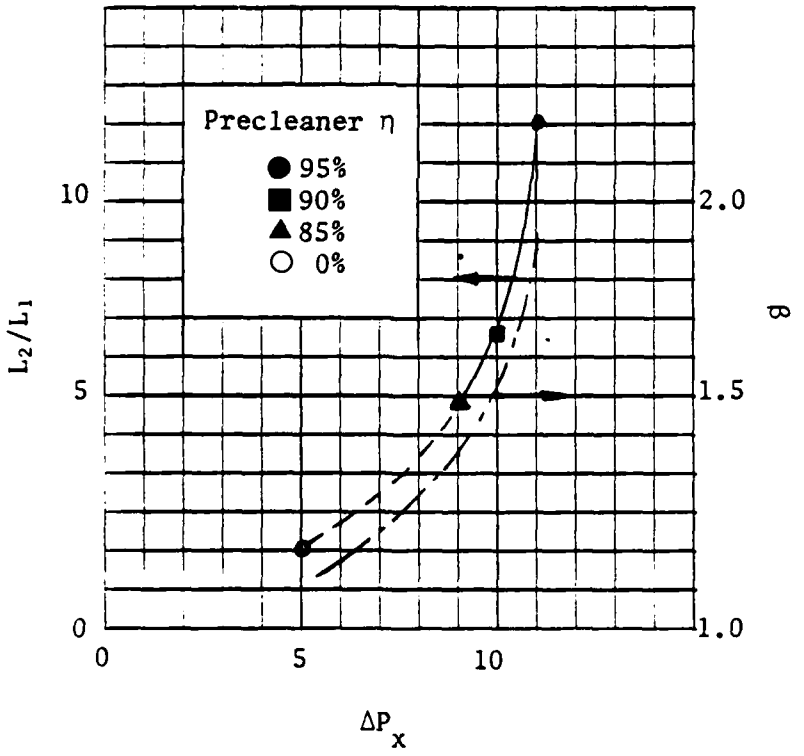

Figure 5-48. L_2/L_1 and β as a Function of ΔP_x Based on Data in Table 5-6.

Table 5-7. Mean Miles Between Vehicle Incidents (MMBVI) and Mean Time Between Vehicle Incidents (MTBVI)

Vehicle	MMBVI (hours)	MTBVI
M48	2159	269
M60	2883	359
M109	4533	453
M110	1642	213
M578	2823	506

Vehicle	Number of Air Cleaners	Number of Blower Motors
M48	2	4
M60	2	4
M728	2	4
M109	1	2
M110	1	2
M551	1	2
M578	1	2

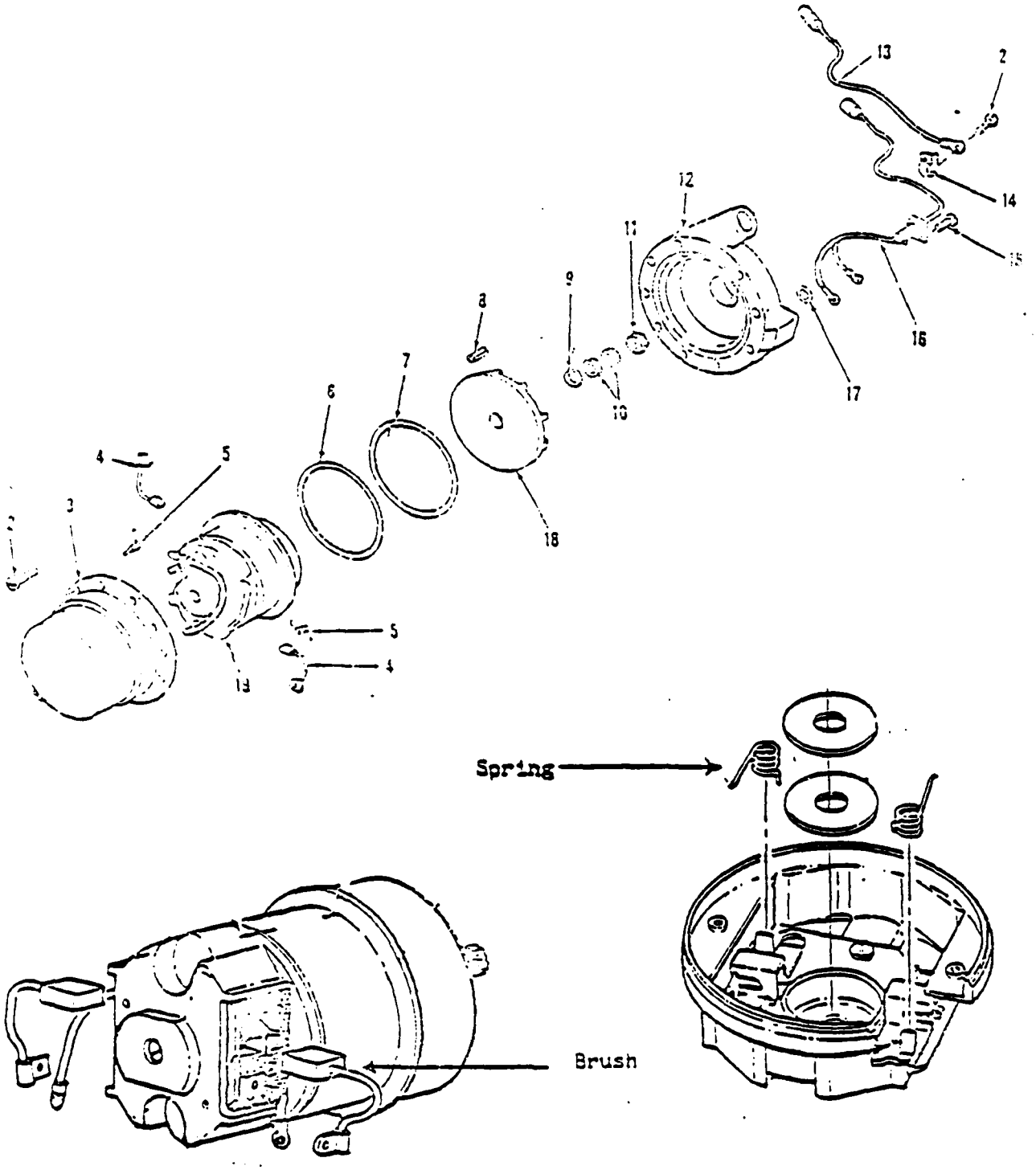

Figure 5-49. Air Cleaner Blower Motor Assembly Used on Several Classes of Tracked Vehicles[1]

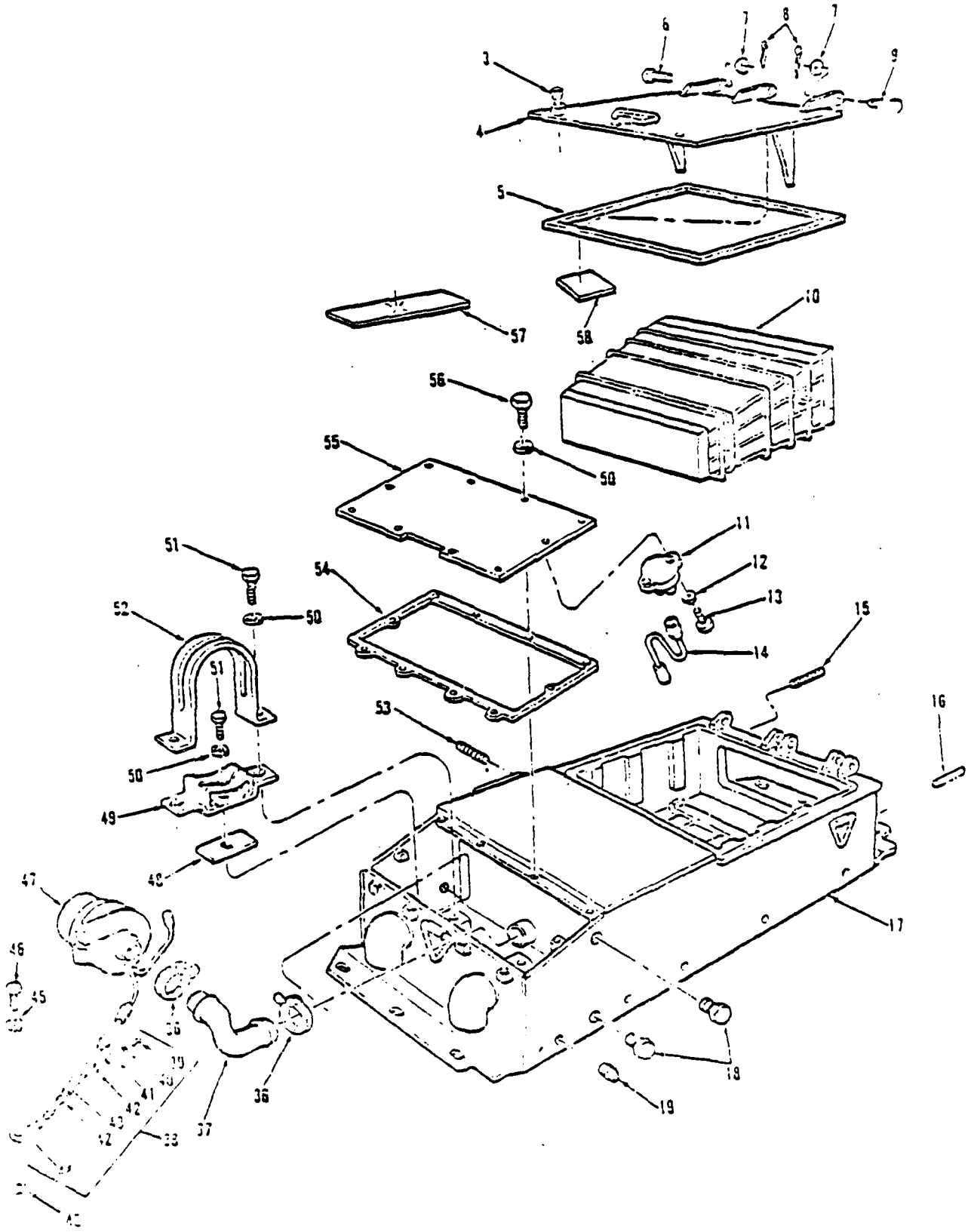

Figure 5-50. Diagram of One of Two Air Cleaners Used on M48, M60, and M728 Vehicles[1]

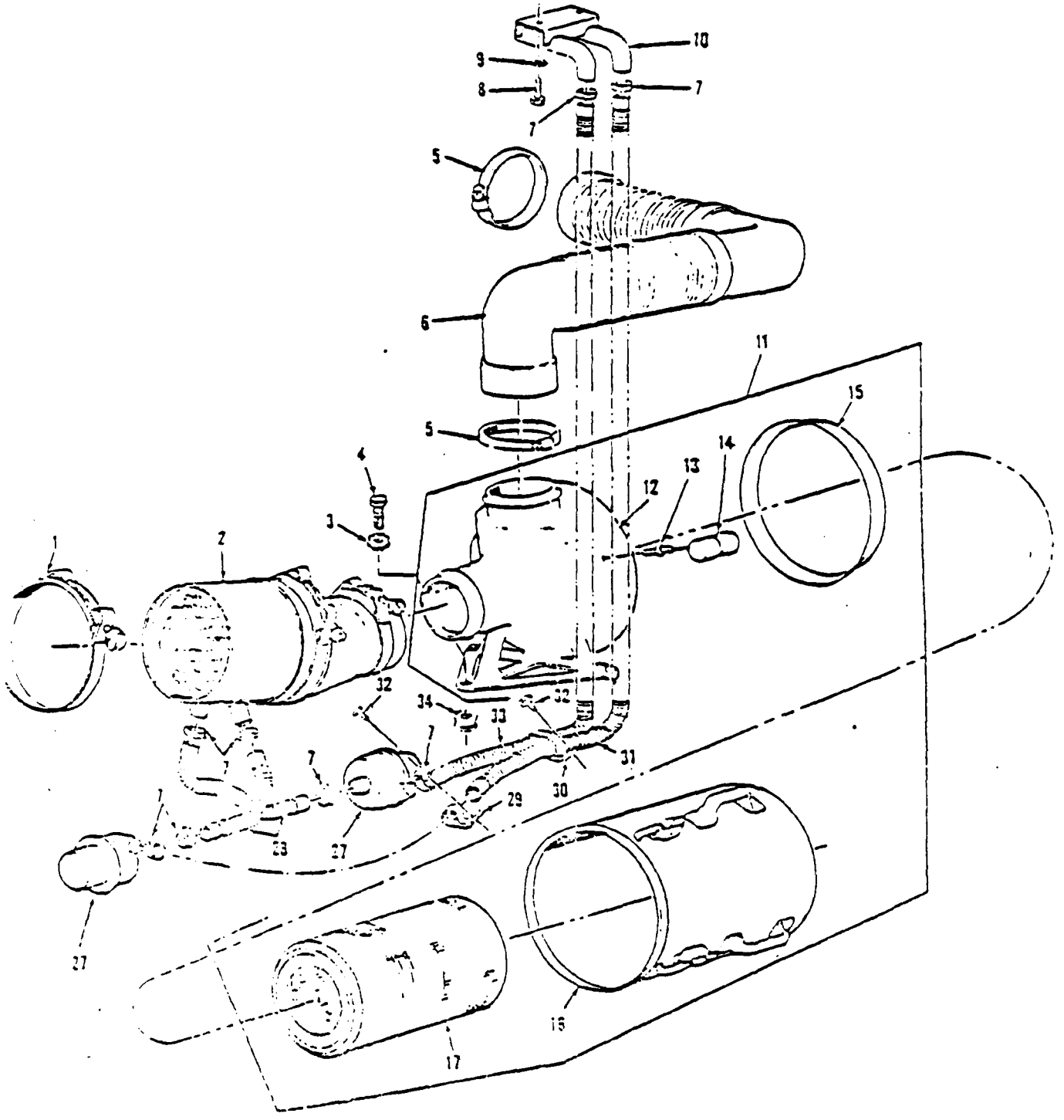

Figure 5-51. Air Cleaner Configuration for the M551 Vehicle[1]

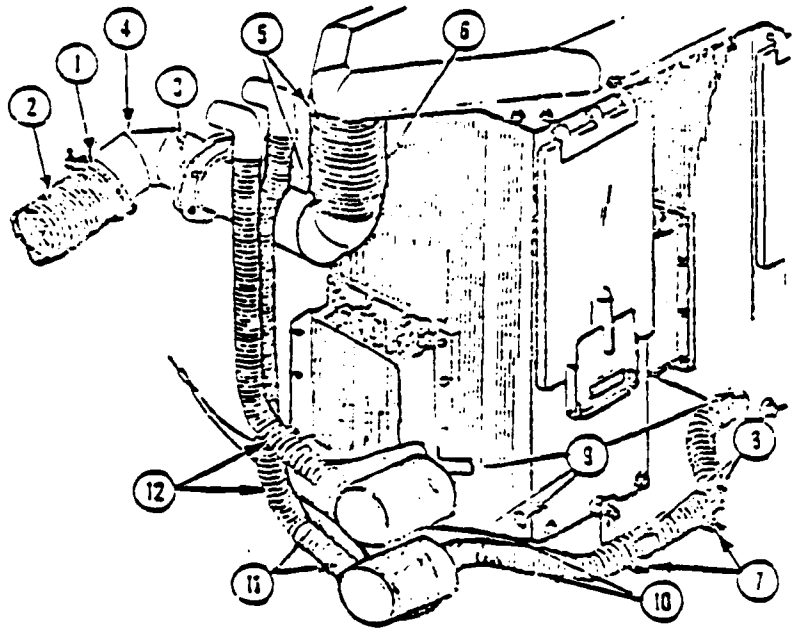

Figure 5-52. Air Cleaner Configuration Used in the M109 Howitzer

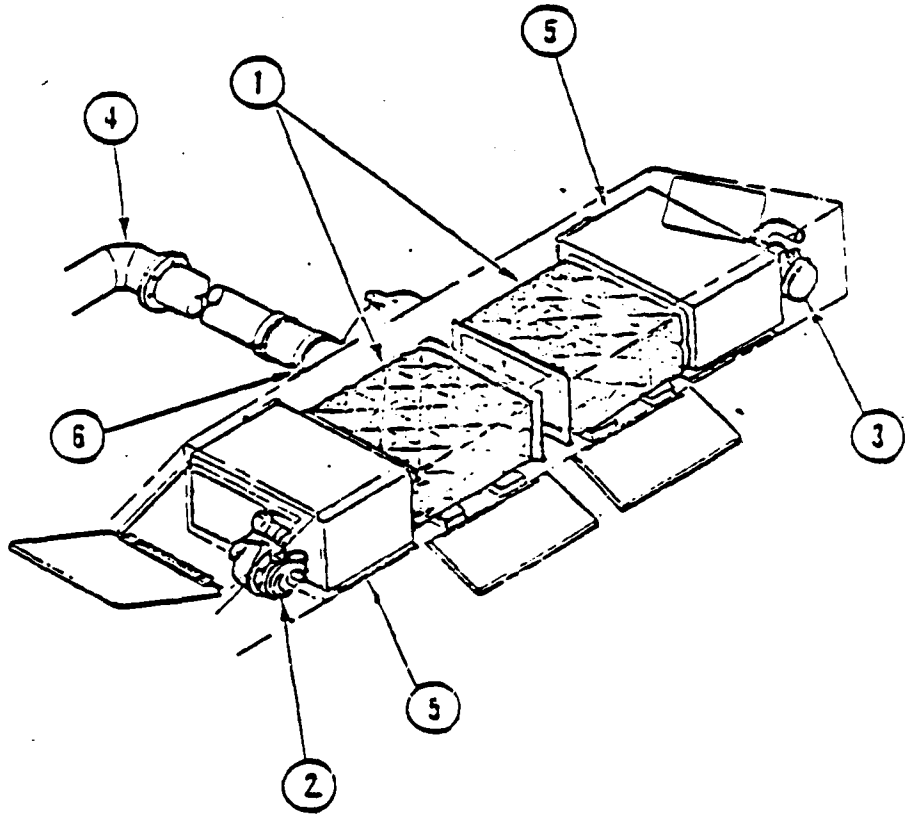

Figure 5-53. Air Cleaner Configuration Used in the M110 Howitzer and the M578 Recovery Vehicle[1]

50 percent of the inlet dust is likely to be removed prior to reaching the filter. The impact of short service life on operations, vehicle performance, and costs are obvious as are the consequences of poor filtration.

The procurement of blower motor assemblies and blower motor repair kits since early 1981 has been significant. In a 17-month period from 15 April 1981 to 28 September 1982, 12,632 blowers were purchased, all from the same contractor. During this time, 12,450 repair kits were also purchased. In 1983, approximately 7,200 units (@ $139 each) were purchased, while in 1984, nearly 10,000 units (@ $118 each) were purchased. Approximately two hours are required to replace an inoperative blower motor assembly, representing an additional cost to the Army. Nearly 3,500 repair kits to replace brushes are purchased per year, while the demand for kits to repair washers and packings was 176 units per month in 1982.

Two actions have been taken to reduce or eliminate the problems encountered with blower motors. First, the blower motor assembly and the First Article Tests were modified in June 1982 in an effort to improve reliability. Second, on certain vehicles (for instance the M60 series tank), blower motors are being replaced with a Vehicle Exhaust Dust Ejection System (VEDES), which uses energy available in the exhaust gases to create a vacuum in the tube leading to the precleaners. As discussed earlier, it is not likely that exhaust gas aspiration will solve all blower motor problems, primarily because of difficulties in placement.

Since the testing and analyses done in this program have shown the fan-airpump is technically feasible for integration into military air cleaner systems, it is important to look at the cost associated with its use. A fan air-pump system, including brackets, clamps and ducting, is estimated to cost $25. Installation should require less than an hour. Since there are no moving parts to wear out, maintenance should be minimal. Inasmuch, the fan-airpump will provide a significant savings based on life cycle cost compared to present-day blower motor systems. Perhaps even more important, however, is the fact that operational readiness could be significantly improved.

LIST OF REFERENCES

1 Cusmano, Ronald, "Air Induction System Blower Motor Study, NSN 4140-00-016-2615, Part No. 10905010," U.S. Army Tank Automotive Command, Warren, Michigan (1983).

DISTRIBUTION LIST

	Copies
Commander U.S. Army Tank-Automotive Command ATTN: DRSTA-RGT Warren, MI 48397-5000	5
Commander U.S. Army Tank-Automotive Command ATTN: DRSTA-TSL Warren, MI 48397-5000	14
DCASMA 615 East Houston Street San Antonio, TX 78294	1

END

FILMED

12-85

DTIC